ILLINOIS STATE WATER SURVEY

at .

University of Illinois
Urbana, Illinois

EXPERIMENTAL AND THEORETICAL INVESTIGATION OF THE COALESCENCE OF LIQUID DROPS.

by

Richard G. Semonin

FINAL SCIENTIFIC REPORT

~~National Science Foundation~~ GP-2528

C Grant

Papers generated by grant research:

1. Cloud droplet collision efficiency in electric fields —— by H. R. Plumlee and R. G. Semonin

2. Collision efficiency of charged cloud droplets in electric fields — by R. G. Semonin and H. R. Plumlee

3. The coalescence delay time: Effects of voltage, velocity, and humidity — by R. G. Semonin.

4. Production of uniform-size liquid droplets —— by N. R. Lindblad and J. M. Schneider

5. An apparatus to study the collision and coalescence of liquid aerosols — by J. M. Schneider, N. R. Lindblad, and C. D. Hendricks

6. On the coalescence and collision of water drops — by R. G. Semonin

7. Effects of electrostatic forces on drop collision and coalescence in air —— (Abstract only) by H. R. Plumlee

February 23, 1967

FINAL SCIENTIFIC REPORT

National Science Foundation GP-2528

EXPERIMENTAL AND THEORETICAL INVESTIGATION OF THE COALESCENCE OF LIQUID DROPS

INTRODUCTION

The objective of the laboratory and theoretical studies summarized in this report is to obtain a better understanding of some of the factors which influence the colloidal stability of liquid particle clouds. The approach followed during the pursuit of this objective was to examine in detail the micro-physical processes which affect the collision and coalescence of water drops.

As more, and more observations of the initial development of precipitation within cumulus clouds become available, it is apparent that the collection mechanism is very important. Even in precipitating clouds, the bulk of the water content is contained in droplets at temperatures well above freezing. It seems likely that the full importance of the warm rain process in mid-latitude clouds is not yet appreciated.

The importance of some of the findings of the research performed during this grant is reported in the following section in summary form. The details of each of the investigations will be found in the Appendices consisting of the published papers resulting from the work accomplished during the preceding two and one-half years.

SUMMARY

Collision Efficiencies

The collection mechanism of droplet growth is considered to be a two-part physical process. The droplets must first collide and then the collision must be

followed by the coalescence of the impacted droplets. The first part of the process requires knowledge of the probability of a collision between a pair of arbitrary size droplets subjected to various aerodynamical, gravitational, and electrical forces.

The collision efficiency.was theoretically determined for several pairs of droplets subjected to the above-mentioned forces. The aerodynamical approximation used in the work was compared with the results obtained by other workers and was found to give reasonable values for the collision efficiencies of the droplet pairs involved. The same pairs of droplets were then assumed to fall in a uniform electric field of varying strength and orientation. The effect of the electric field on the interacting forces between the droplets and the consequences of these forces on the collision probability of the pair are described in Appendices 1 and 7.

In the real atmosphere, however, clouds consist of droplets which carry net. charges which, at least in part, contribute to the electric field within active storms. The problem of calculating the collision efficiencies now becomes considerably more complicated since the additional electrostatic forces due to the interaction of the electric field and the charged particles must be considered. The necessary computations to show these effects were carried out and the results are given in detail in Appendices 2, 6, and 7. The reader is referred to these papers for details and data and especially to Appendix 6 for a summary of the work and an illustrated example, Figure 5, of the results obtained from the calculations.

Coalescence Studies

The above studies on the collision efficiency of droplet pairs were concerned with the. probability of collision as a function of initial separation, relative velocity, electric charge, and electric fields. It is now prudent to inquire as to the probability of coalescence once the droplets have collided.

An experiment was conducted to obtain data on the microphysics of the coalescence process by colliding a pair of drops from hypodermic needles and photographing the profile of the collision with a high speed camera. A battery was connected so that a potential difference from 0 to 10 volts could be developed between the drops. A 10-ohm resistor was placed in series with the battery, and the voltage across the resistor was monitored with an oscilloscope. No voltage was observed, of course, until the two drop surfaces were in physical contact. When charge began to flow in the external circuit, a lamp was lighted and was photographed along the edge of the film. In this way the flow of charge was correlated with the visual coalescence. The results of these observations indicate that there is current between the drops prior to the visual coalescence. Since the voltage between the drops is inadequate to produce ionization of the air, it is hypothesized that the current is an indication of the initial transport of mass and is therefore the initiation of the coalescence process.

The experiment was conducted in an enclosed environment in which the relative humidity, impact velocity, and potential difference between the drops were controlled variables. The results from the experiments show that the voltage is the dominating factor on the time between visual coalescence and actual coalescence for values between 0 and 10 volts. For potential differences in excess of 10 volts, the delay time is independent of the voltage. However, the delay time, then, is dependent on the impact velocity and to a lesser degree on the relative humidity. These results are shown in Appendices 3 and 6. A more detailed discussion of the phenomenon is in preparation for publication in the near future.

Droplet Production Techniques

The study of the interaction of cloud droplets was hindered by the inability to produce droplet pairs of controlled diameter and movement. A device was designed, constructed, and operated which readily produces a stream of uniform size

droplets from a needle. A description of the apparatus is given in Appendix 5. A thorough discussion of the principles of operation of the device is found in Appendix 4. Variations of this principle of droplet production have been used and the entire apparatus is continually undergoing modification as experience is gained with the technique. However, there is a practical limit to the smallest size droplet that can be generated with the device. It appears that the orifice is a serious obstruction to the production of droplets of less than 20 microns in diameter. Additional novel techniques are part of the subject of future laboratory studies of the microphysics of liquid aerosols.

APPENDICES 1 - 7

1. Cloud droplet collision efficiency in electric fields — 16.11-377
   by H. R. Plumlee and R. G. Semonin.

2. Collision efficiency of charged cloud droplets in electric fields -- 18.1-320
   by R. G. Semonin and H. R. Plumlee

3. The coalescence delay time: Effects of voltage, velocity, and humidity —
   by R. G. Semonin No

4. Production of uniform-size liquid droplets —
   by N. R. Lindblad and J. M. Schneider No.

5. An apparatus to study the collision and coalescence of liquid aerosols.—
   by J. M. Schneider, N. R. Lindblad, and C.D. Hendricks No.

6. On the coalescence and collision of water drops -- 17.5-325
   by R. G. Semonin

7. Effects of electrostatic forces on drop collision and coalescence in air —
   (Abstract only) by H. R. Plumlee 16.6-399

Cloud droplet collision efficiency in electric fields

By HUBERT R. PLUMLEE[1] and RICHARD G. SEMONIN,[2] *Charged Particle Research Laboratory, Illinois State Water Survey and University of Illinois, Urbana, Illinois*

(Manuscript received, November 11, 1964)

ABSTRACT

A mathematical model describing the effects of forces acting on two spherical droplets immersed in a viscous medium is described. The model includes the interaction of the droplets with an externally applied electric field. The collision efficiencies between pairs of droplets ranging in size from 5 to 70 microns in radius are given as results of computations of the grazing trajectories of the smaller droplets relative to the larger drops in electric fields up to 10,000 volts per centimeter.

The collision efficiency for a given pair of droplets increases as the applied electric field increases. For example the collision efficiency of a 30 micron drop in relation to a 5 micron droplet increases 34.5 times when the horizontal field is changed from 0 to 3 600 volts per centimeter. Results of calculations are given to show how collision efficiencies vary as the orientation of the electric field is varied in relation to the axis of droplet motion. The results show that the maximum and minimum collision efficiencies occur with field orientations of 90 and 42 degrees respectively.

Introduction

The study of the all-water process of precipitation initiation has led to the concepts of collision, coalescence, and collection efficiencies between droplets of varying size. The collision efficiency is defined as the ratio of the cross-sectional area through which a droplet must pass for a collision to occur with a second droplet to the collision cross-section of the droplet pair. The coalescence efficiency is the fraction of colliding droplets which merge to form a larger drop. The collection efficiency is the product of the collision and coalescence efficiencies.

By the very definition of the coalescence efficiency, it can never exceed but may acquire any value less than or equal to unity. On the other hand, the collision efficiency, theoretically, is unbounded.

The collision efficiency of a pair of droplets is determined by the trajectories of the droplets while they are subjected to gravitational, aerodynamical, and electrical forces. To make the problem tractable for computing collision efficiencies in the presence of electric fields, the coordinate system for the calculation is fixed to the larger droplet (hereafter called the drop). Also it is assumed that the presence of the smaller droplet (hereafter called the droplet) does not disturb the fluid flow around the drop, since the drop-droplet interacting forces are not included. The trajectory of the droplet is determined by integrating the equation of motion

$$m_s \frac{d\mathbf{V}_s}{dt} = \mathbf{F}_a + \mathbf{F}_e + \mathbf{F}_g, \qquad (1)$$

where m_s is the mass of the droplet, V_s is its velocity, F_a is the aerodynamical force, F_e is the electrical force, and F_g is the gravitational force. Theoretical methods are presented whereby each of the forces are determined and the collision efficiencies are obtained as a function of applied electric field.

Definition of collision efficiency

The collision efficiency is a measure of a cross-sectional area such that if the center of a droplet of radius a_s passes through this area the two droplets will collide. The diameter of the cross-sectional area is ascertained by computing

[1] Based upon a portion of a dissertation submitted in partial fulfillment for the degree of Doctor of Philosophy at the University of Illinois.

[2] Co-director, Charged Particle Research Laboratory.

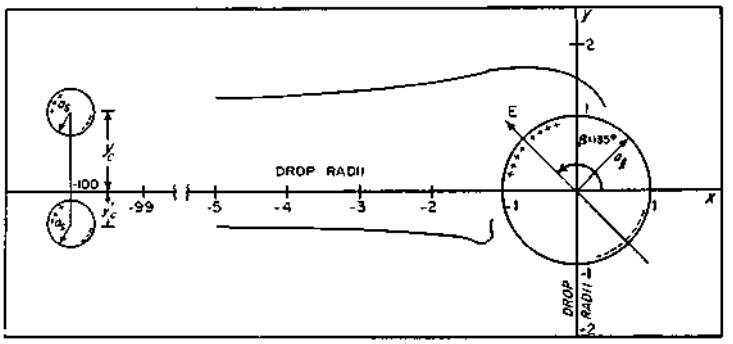

FIG. 1. The grazing trajectories in the half-planes ($y>0$ and $y<0$) for a 30 micron drop and a 5 micron droplet in an electric field oriented at $\beta = 135°$.

a pair of droplet trajectories which graze the collector drop on opposite sides of the axis of fall. The area through which droplets must pass to collide with a drop of radius a_1 is given by

$$\frac{\pi}{4}(y_c - y_c')^2,$$

where y_c is the initial horizontal separation of droplet centers for the grazing trajectory in the upper half-plane of Fig. 1 and y_c is the initial horizontal separation of droplet centers for the grazing trajectories in the lower half-plane. The definition of the collision efficiency, E_c, adopted in this work is the cross-sectional area, determined above, normalized by the collision cross-section of the droplet pair, $(a_l + a_s)^2$. By this definition the collision efficiency is given by

$$E_c = \frac{\pi(y_c - y_c')^2}{4\pi(a_l + a_s)^2}. \tag{2}$$

This definition takes into account non-symmetrical conditions which may occur when electrical forces act on the droplets. In addition, a collision efficiency of unity has a true physical meaning in the above definition. A drop of radius a_l will collide with, all droplets of radius a_s when their centers lie within the drop-droplet pair collision cross-section.

Aerodynamics

The aerodynamical force, F_a, in equation (1) is the drag force on a moving sphere in a viscous medium,

$$\mathbf{F}_a = -6\pi\mu a_s(\mathbf{V}_s - \mathbf{U})\, D_s, \tag{3}$$

where μ is the viscosity of air, a_s is the radius of the droplet, V_s is the droplet velocity at a point in the fluid with velocity U, and D_s is a coefficient to adjust the force for non-Stokesian droplets. The droplet is assumed to be of sufficiently small dimensions so that its effect on the fluid is negligible. The coordinate system is fixed to the drop so that the motions of the droplet and fluid are determined relative to the drop. Fig. 2 illustrates the coordinate system and the components of the forces and velocities shown are directed in the positive direction.

The vector stream velocity U in equation (3) may be written in component form as

$$\mathbf{U} = U_x\hat{x} + U_y\hat{y}, \tag{4}$$

where $\hat{x}$ and $\hat{y}$ are unit vectors. The flow is assumed to be symmetrical about the x-axis.

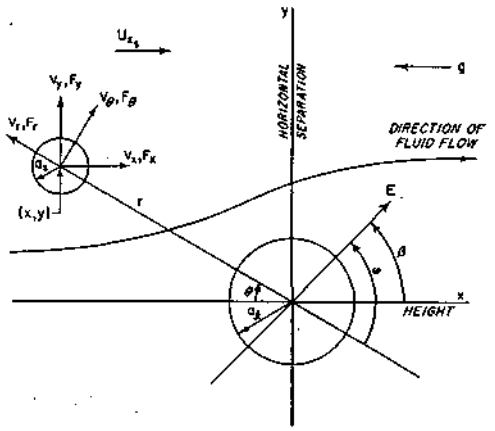

FIG. 2. Motion of a droplet in an electric field, E, relative to a fixed drop.

The r- and θ- components are obtained from the following relationships

$$\left.\begin{aligned} U_x &= -U_r \cos\theta + U_\theta \sin\theta, \\ U_y &= U_r \sin\theta + U_\theta \cos\theta, \end{aligned}\right\} \tag{5}$$

where θ is measured positively in a clockwise direction from the negative x-axis. The angular and radial components of the velocity in terms of a stream function ψ are

$$\left.\begin{aligned} U_r &= -\frac{1}{r^2 \sin\theta}\frac{\partial\psi}{\partial\theta}, \\ U_\theta &= \frac{1}{r\sin\theta}\frac{\partial\psi}{\partial r}. \end{aligned}\right\} \tag{6}$$

The stream function derived by PROUDMAN and PEARSON (1957) as a compromise between the OSEEN (1910) solution which satisfies the farfield boundary conditions and the STOKES (1851) solution which satisfies the no-slip condition at the surface of the sphere is used in this work. The stream function in terms of the Reynolds number, R_e, of the drop is given as

$$\begin{aligned} \psi = \frac{U_\infty}{4}\left(\frac{r}{a_1}-1\right)^2 (1-\cos^2\theta) \\ \cdot\left[\left(1+\frac{3R_e}{16}\right)\left(2+\frac{a_1}{r}\right)-\frac{3R_e}{16}\right. \\ \left.\cdot\left(2+\frac{a_1}{r}+\frac{a_1^2}{r^2}\right)\cos\theta\right], \end{aligned} \tag{7}$$

where r is the radius vector to the point (r, θ) in the fluid, and U_{oo} is the undisturbed fluid flow. The Reynolds number is defined as $2\varrho_a U_{oo}\, a_1/\mu$ where ϱ_a is the density of air at 20° C and standard pressure, and the other symbols are as defined previously. When the partial derivatives of this expression are substituted in equation (6), the velocity components are found to be

$$\left.\begin{aligned} U_r = \frac{U_\infty}{4}\left(1-\frac{a_1}{r}\right)^2\left[(1-3\cos^2\theta)\right. \\ \cdot\left(2+\frac{a_1}{r}+\frac{a_1^2}{r^2}\right)\frac{3R_e}{16}+2\cos\theta \\ \left.\cdot\left(1+\frac{3R_e}{16}\right)\left(2+\frac{a_1}{r}\right)\right], \end{aligned}\right\} \tag{8}$$

$$\left.\begin{aligned} U_\theta = \frac{U_\infty}{4}\sin\theta\left(1-\frac{a_1}{r}\right)\left[\left(1+\frac{3R_e}{16}\right)\right. \\ \cdot\left(4+\frac{a_1}{r}+\frac{a_1^2}{r^2}\right)-\frac{3R_e}{16} \\ \left.\cdot\left(4+\frac{a_1}{r}-\frac{2a_1^3}{r^3}\right)\cos\theta\right]. \end{aligned}\right\} \tag{8}$$

The aerodynamical force necessary to obtain the trajectories from equation (1) is obtained by substituting equation (8) into the angular and radial component form of equation (3). The x- and y- components are given as

$$\left.\begin{aligned} F_{xa} &= -F_{ra}\cos\theta + F_{\theta a}\sin\theta, \\ F_{ya} &= F_{ra}\sin\theta + F_{\theta a}\cos\theta, \end{aligned}\right\} \tag{9}$$

which is the form most convenient for computer use.

As discussed in the foregoing, the problem of two moving spheres was simplified by assuming that the fluid containing the droplet was flowing around a stationary drop. To solve the two-body problem, it was necessary to determine the flow of the fluid around the droplet. HOCKING (1959) estimated that the ratio of droplet radius to drop radius should be approximately one-tenth or less so that the mutual interaction of the flow patterns could be neglected. A comparison of the collision efficiencies of the present work with Hocking's and with SHAFRIR and NEIBURGER'S (1963) is presented in Fig. 3 and shows that the ratio of one-tenth is more conservative than necessary for most cloud physics considerations.

Electrostatics

If water droplets are considered to be conducting spheres, the derivation of the electrostatic forces acting on them is simplified. Since the droplets to be considered are small and travel at moderate velocities, the assumption of the droplets being spheres will introduce only a small error in the results. From the equation of continuity of charge, $\nabla\cdot\mathbf{J}+\partial\varrho_\omega/\partial t=0$, where J is the current density and ϱ_w is the charge density in the water, the relaxation time of the charge distribution in water can be derived in the following manner. Since $J=\sigma E$ where σ is the conductivity of water, then the continuity equation reduces to $\sigma\nabla\cdot\mathbf{E}+\partial\varrho_\omega/\partial t=0$. But

$\nabla \cdot \mathbf{E} = \varrho_w/\varepsilon$ where E is the permittivity of water; therefore, $\sigma\varrho_w/\varepsilon + \partial\varrho_w/\partial t = 0$. The charge density is proportional to exp $(-\sigma t/\varepsilon)$ where the time constant, ε/σ, is the relaxation time for charge transfer in the material. For distilled water, the relaxation time is of the order of 100 microseconds. The charge density, thus the electric field intensity within the drop, decreases rapidly to zero with increasing time. This expresses the well-known fact that the field within a conductor is zero and justifies the assumption that water can be considered to be a conducting material.

DAVIS (1964) solved for the forces acting on two conducting rigid spheres when a uniform electric field, E, is present. He used a bispherical coordinate system as described by MORSE and FESHBACH (1953) and determined the surface charge densities, σ_s and Σ_l, on the conducting spheres. The force acting on the droplet in the MKS system of units was computed by integrating the surface stress $\sigma_s^2/2\varepsilon_0$ over the surface of the droplet where ε_0 is the permittivity of free space.

The force on the droplet written in a convenient form for programming on a digital computer is given by

$$\mathbf{F}_e = F_{xe}\hat{x} + F_{ye}\hat{y}, \tag{10}$$

where
$$\left.\begin{aligned} F_{xe} &= -F_{re}\cos\theta + F_{\theta e}\sin\theta, \\ F_{ye} &= F_{re}\sin\theta + F_{\theta e}\cos\theta. \end{aligned}\right\} \tag{11}$$

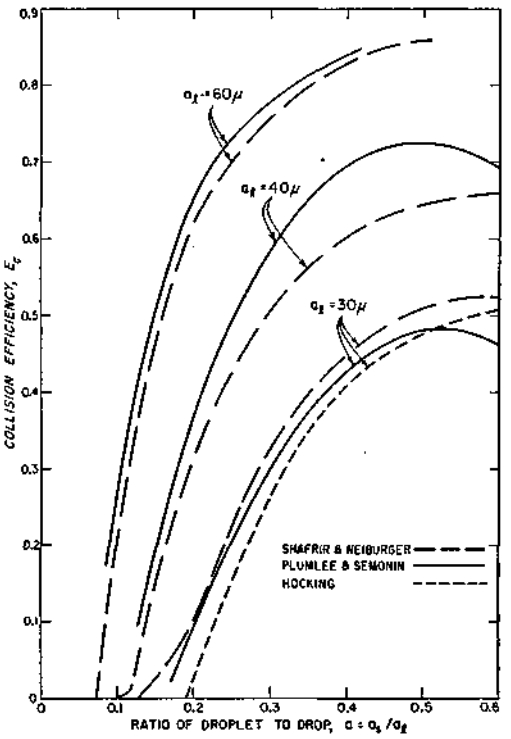

FIG. 3. Comparison of collision efficiencies as calculated by various authors.

From the rearranging of Davis' solutions of the smaller sphere, the components of the force acting in the *r*- and θ- directions are given by

$$\left.\begin{aligned} F_{re} &= 4\pi\varepsilon_0 A^2 \sum_{n=0}^{\infty} S_n\{(2n+1)S_n - (n+1)[\exp(2\mu_s)+1]S_{n+1}\}\exp[(2n+1)\mu_s] \\ &+ 8\pi\varepsilon_0 A^2 E^2 \sin^2\omega \sum_{n=0}^{\infty} n(n+1)\,T_n\{(2n+1)\,T_n - (n+2)[\exp(2\mu_s)+1]\,T_{n+1}\}\exp[(2n+1)\,\mu_s], \\ F_{\theta e} &= 4\pi\varepsilon_0 A^2 E \sin\omega[\exp(2\mu_s)-1]\sum_{n=0}^{\infty}(n+1)\{nS_{n+1}T_n - (n+2)S_n T_{n+1}\}\exp[(2n+1)\mu_s]. \end{aligned}\right\} \tag{12}$$

The coefficients are given as

$$\left.\begin{aligned} S_n &= \frac{E(2n+1)\cos\omega\left\{\exp[(2n+1)\mu_l+1] - \left(\frac{\phi_s}{A}\right)\right\}\exp[(2n+1)\mu_l] + \left(\frac{\phi_l}{A}\right)}{\exp[(2n+1)\mu_0]-1}, \\ T_n &= \frac{1-\exp[(2n+1)\mu_l]}{1-\exp[(2n+1)\mu_0]}. \end{aligned}\right\} \tag{13}$$

The potentials of each sphere due to both the induced charges, Q_l and Q_s, and the net charges, q_l and q_s, are

$$\left.\begin{aligned}\phi_l &= P_{ll}(q_l - 8\pi\varepsilon_0 A^2 EQ_l \cos\omega) + P_{ls} \\ &\quad \cdot (q_s - 8\pi\varepsilon_0 A^2 EQ_s \cos\omega), \\ \phi_s &= P_{sl}(q_l - 8\pi\varepsilon_0 A^2 EQ_l \cos\omega) + P_{ss} \\ &\quad \cdot (q_s - 8\pi\varepsilon_0 A^2 EQ_s \cos\omega).\end{aligned}\right\} \quad (14)$$

The coefficients of induction are

$$\left.\begin{aligned}P_{ll} &= \frac{C_{ss}}{C_{ll}C_{ss} - C_{ls}^2}, \\ P_{ls} = P_{sl} &= \frac{C_{ls}}{C_{ll}C_{ss} - C_{ls}^2}, \\ P_{ss} &= \frac{C_{ll}}{C_{ll}C_{ss} - C_{ls}^2},\end{aligned}\right\} \quad (15)$$

where the coefficients of capacitance are

$$\left.\begin{aligned}C_{ll} &= 8\pi\varepsilon_0 A \sum_{n=0}^{\infty} \frac{\exp[(2n+1)\mu_s]}{\exp[(2n+1)\mu_0] - 1}, \\ C_{ls} = C_{sl} &= 8\pi\varepsilon_0 A \sum_{n=0}^{\infty} \frac{1}{\exp[(2n+1)\mu_0] - 1}, \\ C_{ss} &= 8\pi\varepsilon_0 A \sum_{n=0}^{\infty} \frac{\exp[(2n+1)\mu_l]}{\exp[(2n+1)\mu_0] - 1}.\end{aligned}\right\} \quad (16)$$

The induced charges are

$$\left.\begin{aligned}Q_l &= 8\pi\varepsilon_0 A^2 \sum_{n=0}^{\infty} (2n+1) \frac{\exp[(2n+1)\mu_s] + 1}{\exp[(2n+1)\mu_0] - 1}, \\ Q_s &= -8\pi\varepsilon_0 A^2 \sum_{n=0}^{\infty} (2n+1) \\ &\quad \cdot \frac{\exp[(2n+1)\mu_l] + 1}{\exp[(2n+1)\mu_0] - 1},\end{aligned}\right\} \quad (17)$$

where

$$\left.\begin{aligned}&\exp(\mu_l) = \frac{C_l + A}{a_l}; \quad \exp(\mu_s) = \frac{C_s + A}{a_s} \\ &\mu_0 = \mu_l + \mu_s \\ &A = (C_l^2 - a_l^2)^{\frac{1}{2}} \\ &C_l = (r^2 + a_l^2 - a_s^2)/2r \\ &C_s = (r^2 + a_s^2 - a_l^2)/2r\end{aligned}\right\} \quad (18)$$

In the above equations, E is the applied electric field, w is the angle between the electric field and the line joining the centers as illustrated in Fig. 2, and q_l and q_s are the net charges on the drop and droplet respectively. For the work reported here, the droplets are uncharged and q_l and q_s are zero.

Equations of motion

The various forces acting on the droplet are determined from the foregoing analyses. Since the negative x-axis is selected as the direction of vertical fall, the gravitational force, $m_s g$, acts on the droplet in the negative x-direction as shown in Fig. 2.

The equations of motion including the various forces are written in component form as

$$\left.\begin{aligned}m_s \frac{dV_{xs}}{dt} &= -6\pi\mu a_s (V_{xs} - U_x) D_s - m_s g + F_{xe}, \\ m_s \frac{dV_{ys}}{dt} &= -6\pi\mu a_s (V_{ys} - U_y) D_s + F_{ye}, \\ \frac{dx_s}{dt} &= V_{xs}, \\ \frac{dy_s}{dt} &= V_{ys}.\end{aligned}\right\} \quad (19)$$

These equations of motion were solved by the use of a digital computer and a numerical integrating routine first described by NORDSIECK (1962). The routine incorporated automatic starting and automatic selection and revision of the integration step. To start the integration, only the initial conditions, a specified accuracy of integration, and a logical elementary integration step are necessary. At small distances from the drop where changes in the motion of the droplet are greatest, the integration step is automatically shortened to obtain a solution of the given accuracy.

The initial velocities of the drop and droplet are determined by computing the terminal velocity of each when gravity acts on the masses. Since the center of the drop is assumed as the origin of a fixed coordinate system, the initial velocity of the droplet is the difference between the terminal velocities of the two droplets. The initial vertical separation for each trajectory is taken as 100 drop radii. At this separation, there is very little interaction between the disturbed fluid around the drop and the droplet. The initial horizontal separation ,of the first trajectory is taken as one drop radius.

Discussion of results

The collision efficiencies for pairs of droplets when either a horizontal or a vertical electric field is present are shown in Figs. 4, 5, and 6. The increase in the collision efficiency due to an applied electric field is a result of an induced nonuniform charge distribution on the surfaces of the two droplets. The interaction of the two charge distributions can either be attractive or repulsive depending on the orientation of the applied field and the relative position of the droplets. If only the dipole interaction is considered, the regions of attraction and repulsion can be determined as illustrated by LINDBLAD and SEMONTN (1963).

The results given in Figs. 4, 5, and 6 show that the influence of the fair weather atmospheric electric field cannot contribute to the collision efficiency of the drop-droplet pairs considered in this study. The normal fair weather electric field is of the order of one volt per centimeter whereas the major changes in the efficiency of collision occur at electric field intensities which are orders of magnitude greater.

The trajectories for the 30 and 5 micron droplet pair are shown in Fig. 7. The effect of

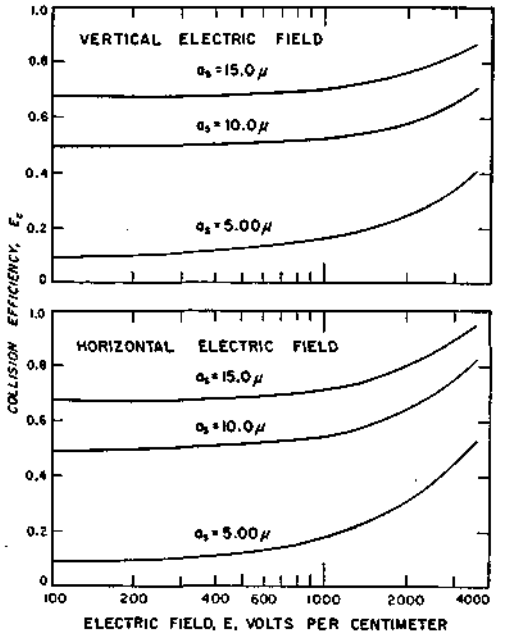

FIG. 5. Collision efficiency curves for a 40 micron drop with 5, 10, and 15 micron droplets.

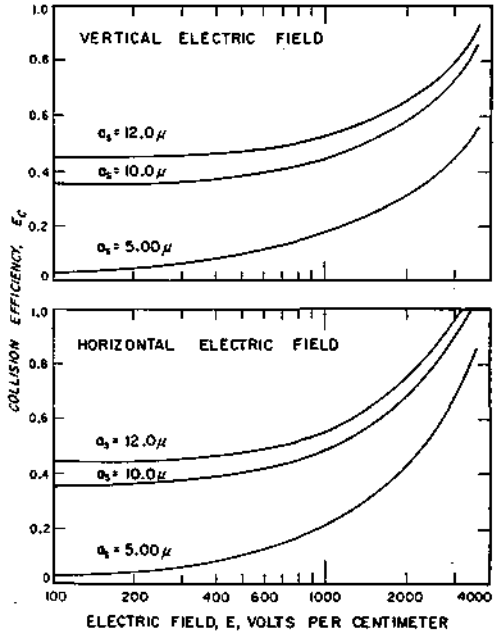

FIG. 4. Collision efficiency curves for a 30 micron drop with 5, 10, and 12 micron droplets.

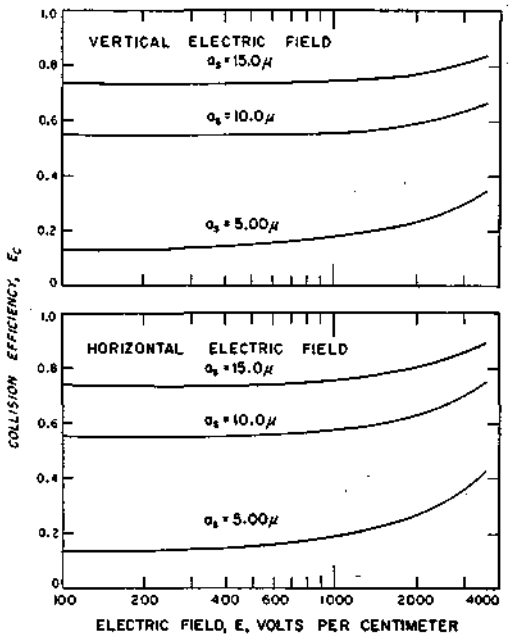

FIG. 6. Collision efficiency curves for a 50 micron drop with 5, 10, and 15 micron droplets.

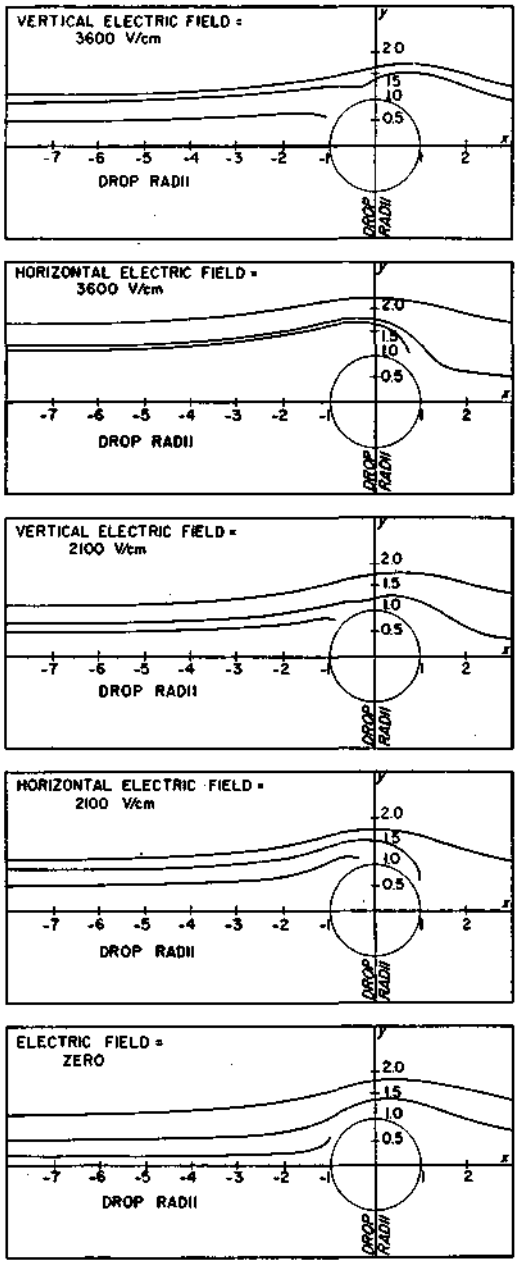

FIG. 7. Trajectories for a 5 micron droplet moving toward a 30 micron drop.

a region of repulsion about the *y*-axis on the trajectories is illustrated for the case of vertically applied electric fields. The initial trajectory of the droplet is toward the drop but it changes its direction of travel after entering this region of repulsion. The horizontally applied electric fields have a region of attraction about the *y*-axis and result in pulling the droplet into the back side of the drop for certain initial conditions of the droplet.

It is observed from Figs. 4, 5, and 6 that the horizontally applied electric fields produce the largest increase in collision efficiencies and the efficiencies are greatest for the 30 and 5 micron droplet pair. A horizontal electric field of 3 600 volts per centimeter increases the collision efficiency of a 30 and 5 micron pair by a factor of 34.5 compared to 5.6 for the 40 and 5 micron pair and 5.0 for the 50 and 5 micron pair. Thus, the collision efficiency curves flatten as the collector drop increases in size. This is due to the large difference between the relative velocities of the drop and droplet which does not allow a sufficient time for the electrical force to bring the pair together.

The effect of the orientation of the applied electric field is seen in Figs. 8 and 9 which show the change in the collision efficiency for various droplet pairs as a function of the angle β between the electric field, E, and the x-axis. The angle β in Fig. 2, is measured positively in the counterclockwise direction and the effects are symmetric for an orientation about the *y*-axis where β is equal to either 90° or 270°. The largest collision efficiencies occur approximately in the range $50° < \beta \leq 90°$ and the lowest collision efficiency occurs for β approximately equal to 42°. The maximum collision efficiency occurs

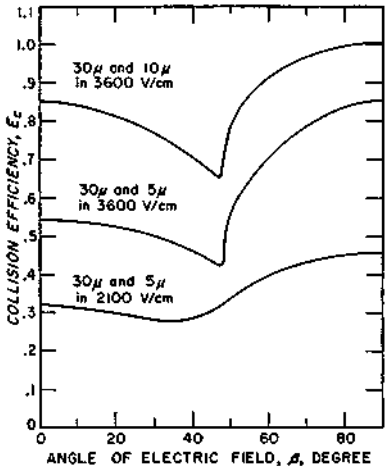

FIG. 8. Change in collision efficiency of droplet pairs for various orientations of electric fields.

TABLE 1. *Collision efficiencies for droplets for strong electric fields.*

Droplet Pair	Vertical Field			Horizontal Field		
	3 600V/cm	6 OOOV/cm	10,000V/cm	3 600V/cm	6 OOOV/cm	10,000V/cm
30μ and 5μ	0.5475	0.9624	1.7315	0.8540	1.4935	2.747
40μ and 5μ	0.4038	0.6433	1.0923	0.5368	0.8854	1.5190
50μ and 5μ	0.3433	0.5095	0.8200	0.4316	0.6729	1.0974

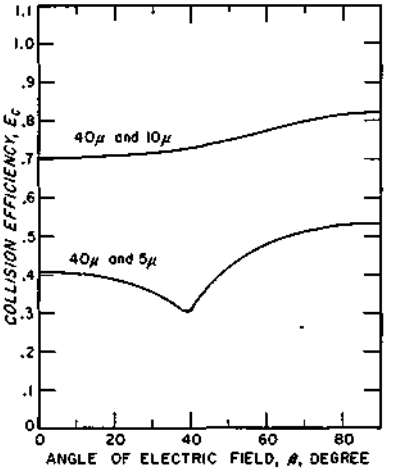

FIG. 9. Change in collision efficiency of droplet pairs for various orientations of electric fields at 3 600 volts per centimeter.

for β equal to 90°, i. e., a horizontally applied electric field.

Collision efficiencies for electric fields of 6 000 and 10,000 volts per centimeter are given in Table 1. For these very large electric fields, collision efficiencies greater than unity are calculated. Although such large fields are not commonly measured in clouds, it does seem reasonable that they may exist in very active clouds where lightning is present.

Conclusions

The collision efficiencies for uncharged cloud droplets of the sizes considered increase with an applied electric field. The maximum increase results for /? equal to 90°, i. e., a horizontally applied electric field and the minimum increase results for β equal to 42°. For a given droplet size with or without electric fields present, the collision efficiency decreases as the drop size increases. However, for a given drop size the collision efficiency increases as the droplet size increases. If the strength of the applied electric field becomes high enough, the collision of cloud droplets can exceed unity.

Acknowledgements

We would like to acknowledge the assistance of Mr. E. Hassler, and Mr. N. Lindblad for discussions during the initial formulation of the problem. Special thanks are due Professor C. D. Hendricks, Co-Director CPRL who acted as thesis advisor for one of us.

This work was supported by U. S. Army Electronic Research and Development Laboratory grant AMC-63-G2 and National Science Foundation Grant NSF-GP2528. The use of the University of Illinois 7094-1401 computing system was partially supported by National Science Foundation grant NSF-GP700.

REFERENCES

DAVIS, M. H., 1964, Two Charged Spherical Conductors in a Uniform Electric Field; Forces and Field Strength, *Quart. J. of Mech. and Appl. Math.*, Vol. 17, Pt. 4, p. 499.

HOCKING, L. M., 1959, Three-dimensional Viscous Flow Problems Solved by the Stokes and Oseen approximation, *Ph. D. Thesis,* 100 pp. *University of London.*

LINDBLAD, N. R., and SEMONIN, R. G., 1963, Collision Efficiency of Cloud Droplets in Electric Fields, *J. of Geophys. Research,* Vol. 68, No. 4, p. 1051.

MORSE, P. M., and FESHBACH, H., 1953, Methods of Theoretical Physics, *McGraw-Hill Book Company, Inc.,* New York, p. 665 and 1298.

NORDSIECK, A. T., 1962, On Numerical Integration of Ordinary Differential Equations, *Math. Computation,* Vol. 16, p. 22.

OSEEN, C. W., 1910, Über die Stokessche Formel und ü ber eine verwandte Aufgabe in der Hydrodynamik, *Ark. Mat. Astr. Fys.,* Vol. 6, No. 29, p. 175.

PROUDMAN, I., and PEARSON, J. R. A., 1957, Expansions at Small Reynolds Numbers for the Flow Past a Sphere and a Circular Cylinder, *Journ. of Fluid Mech.,* Vol. 2, p. 237.

SHAFRIR, U., and NEIBURGER, M., 1963, Collision Efficiencies of Two Spheres Falling in a Viscous Medium, *J. of Geophys. Oesearch,* Vol. 68, No. 13, p. 4141.

STOKES, G. G., 1851, On the Effect of the Internal Friction of Fluids on the Motion of Pendulums, *Transactions, Cambridge Phil. Soc,* Vol. IX, Pt. II, p. 8.

Collision Efficiency of Charged Cloud Droplets in Electric Fields

R. G. SEMONIN AND H. R. PLUMLEE[1,2]

Illinois State Water Survey and University oj Illinois, Urbana

Collision efficiencies are shown for 5- and 10-micron droplets colliding with 30-, 40-, and 50-micron drops. The charge on the drop is always positive, but the sign of the charge on the droplet is alternately positive and negative. The magnitude of the charge on the droplet extends from zero to 10^{-14} coulomb. The calculations are also extended to include electric field intensities of 0, 900, 2100, and 3600 v/cm oriented at angles of 0°, 90°, and 180° with respect to the direction of fall of the drop. The electrical effects were found to influence collision efficiencies only when the droplet charges were greater than about 10^{-16} coulomb or when the electric field intensity exceeded 900 v/cm. The pertinence of the calculations to the physics of electrified clouds is briefly discussed.

INTRODUCTION

The growth of cloud droplets to precipitation particles within clouds free of ice is dependent upon the condensation and evaporation of water vapor and, more importantly, upon the rate at which collisions occur between droplets. The collision rate between droplets is dependent upon the forces acting on or between the spheres. These forces may be due to gravity, a viscous environment, or electrostatic fields. *Fletcher* [1962], in a study of the effects of electrical charges and environmental static fields on the initial development of clouds, concluded that the normal atmospheric electric fields and droplet charges are too small to influence the colloidal stability of the droplet population within a cloud and that the collision rate between droplets in such clouds is therefore determined primarily by gravitational and aerodynamical forces.

In the later stages of development of a cloud, however, appreciable electrical charges and environmental static fields may exist. *Sartor* [1960] theoretically demonstrated that for selected droplet pairs the collision efficiency for normally noncolliding droplets becomes finite in the presence of electrostatic fields of only 10 to 30 v/cm. *Krasnogorskaya* [1965] has also shown that the collision efficiency of normally noncolliding droplets becomes finite with increasing charge and/or electric field. Examples were presented indicating that even with charges of the same sign collisions occur as the result of electrical image forces. *Moore et al.* [1964] have observed many stationary thunderstorms in New Mexico and have concluded from their study of rain gushes that electrical charges and fields predominate in the enhancement of precipitation after a lightning discharge.

Lindblad and Semonin [1963] discussed the effects of an external electric field on the collision efficiencies of cloud droplets. The simple dipole model of induced charge distribution used in their work consistently resulted in increases of collision efficiencies for droplets ranging in radius from 30 to 50 μ in collision with droplets ranging from 5 to 15 μ in radius. *Plumlee and Semonin* [1965], using a more general solution for the electrostatic forces, obtained similar results. The collision efficiencies calculated by Plumlee and Semonin yielded somewhat greater values because of the inclusion of additional multipole terms in determining the electrostatic forces. However, in both of the above papers the droplets were considered to be uncharged. In the following report we consider the effects of electric fields on the collision efficiency of charged droplets.

GENERAL APPROACH TO THE PROBLEM

The collision efficiency of a pair of droplets is determined by the trajectories of the drop-

[1] Now at Texas Instruments, Inc., Dallas, Texas.

[2] Based upon part of a dissertation submitted in partial fulfillment of the requirements for the Ph.D. degree in Electrical Engineering at the University of Illinois.

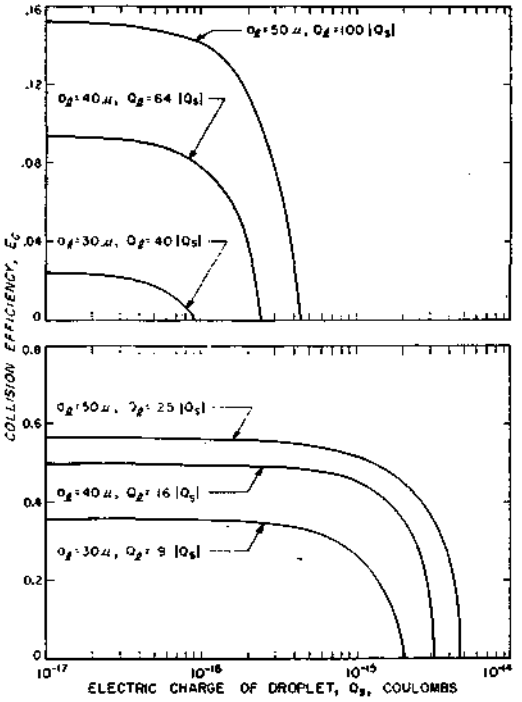

Fig. 1. Collision efficiency curves for a 5-μ (above) and 10-μ (below) droplet with a 30-, 40-, and 50-μ drop.

lets while subjected to gravitational, aerodynamical, and electrical forces. A mathematical model of the collision process can be developed only through the use of judicious approximations to the various forces involved. The equations, assumptions, and definitions used in this work have recently been described by *Plumlee and Semonin* [1965]. The mathematical approach used in the determination of the collision efficiency of charged cloud droplets is identical with that used by Plumlee and Semonin, with the important exception that net charges on the droplet pairs are considered. The definition of a collision as used in this work has been previously discussed by *Lindblad and Semonin* [1963].

The equations of motion for charged droplets falling at terminal velocity including the various forces are written in component form as

$$m_s \frac{dV_{xs}}{dt} = -6\pi\mu a_s(V_{xs} - U_x)D_s - m_s g + F_{xs}$$

$$m_s \frac{dV_{ys}}{dt} = -6\pi\mu a_s(V_{ys} - U_y)D_s + F_{ys}$$

$$dx_s/dt = V_{xs}$$

$$dy_s/dt = V_{ys}$$

where m_s, V, a_s, and D_s are the mass, velocity, radius, and drag coefficient of the droplet and μ, U, g, and F are the viscosity, free-stream velocity, gravity, and total electrostatic force acting on the droplet. These equations of motion were solved by the use of a digital computer and a numerical integrating routine first described by *Nordsieck* [1962]. The routine is so programmed that the integration steps are automatically started, selected, and revised. To start the integration, only the initial conditions, a specified accuracy of integration, and a logical elementary integration step are necessary. At small distances from the drop, where changes in the motion of the droplet are greatest, the integration step is automatically shortened to obtain a solution of the given accuracy.

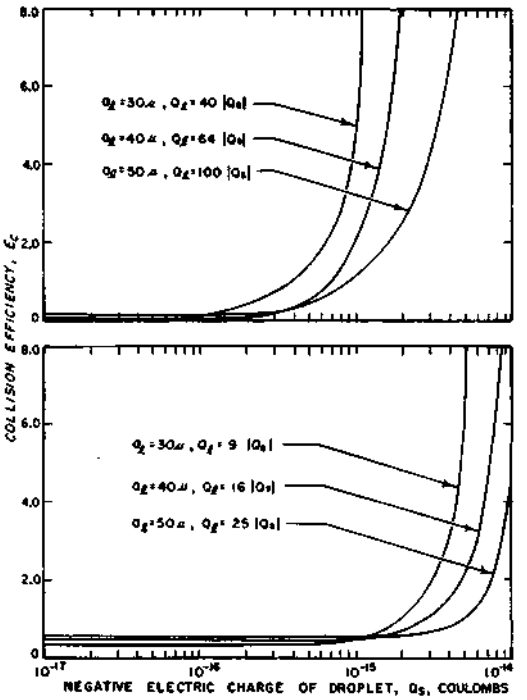

Fig. 2. Collision efficiency curves for a 5-μ (above) and 10-μ (below) droplet with a 30-, 40-, and 50-μ drop.

The initial velocities of the drop and droplet are determined by computing the terminal velocity of each under the influence of gravity and electric fields. Since the center of the drop is assumed to be the center of a fixed coordinate system, the initial velocity of the droplet is the difference between the terminal velocities of the drop and droplet. The initial vertical separation for each trajectory is taken as 100 drop radii. At this separation, the interaction between the disturbed fluid around the drop and the droplet is negligible. The initial horizontal separation of the first trajectory is taken as 1 drop radius.

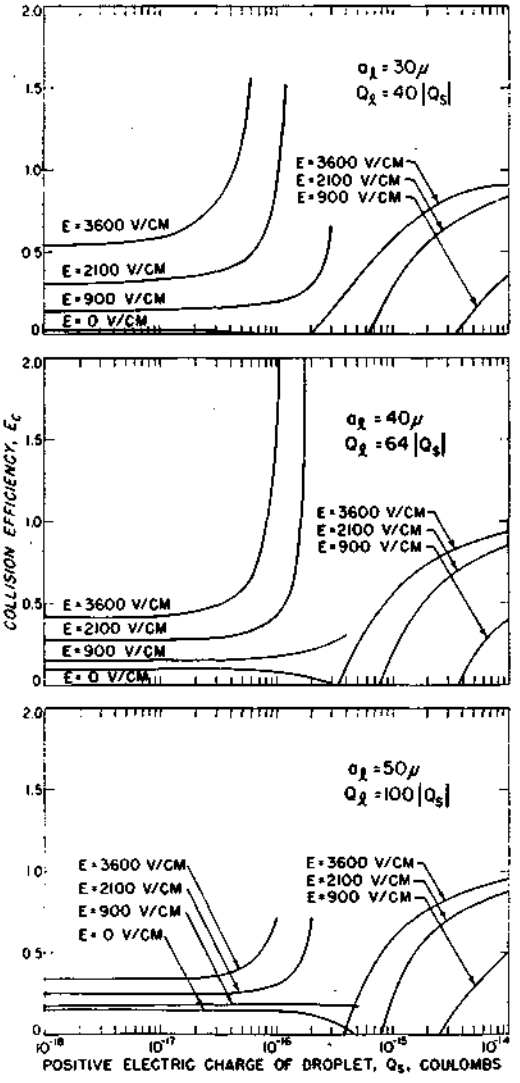

Fig. 3. Collision efficiency curves for a positively charged 5-μ droplet colliding with a 30-, 40-, and 50-μ drop in electric fields oriented at $\beta = 0^o$

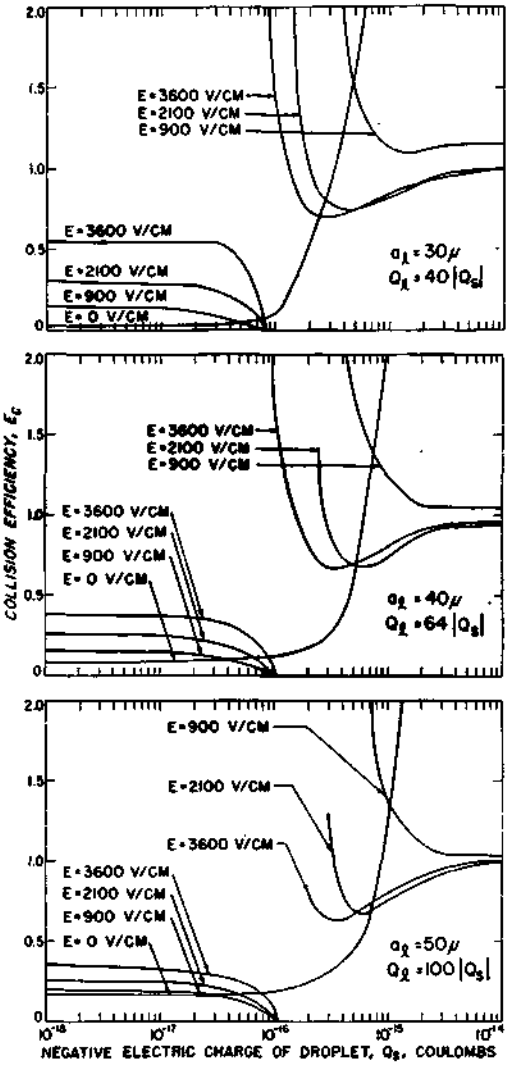

Fig. 4. Collision efficiency curves for a negatively charged 5-μ droplet colliding with a 30-, 40-, and 50-μ drop in electric fields oriented at $\beta = 0^o$.

The charge on the drop is arbitrarily selected to be always positive, since only the magnitudes and relative signs of the charges on a drop-droplet pair are important in determining their collision efficiencies. Obviously there is an infinite number of possible combinations of drop-droplet charge magnitudes that could be con-

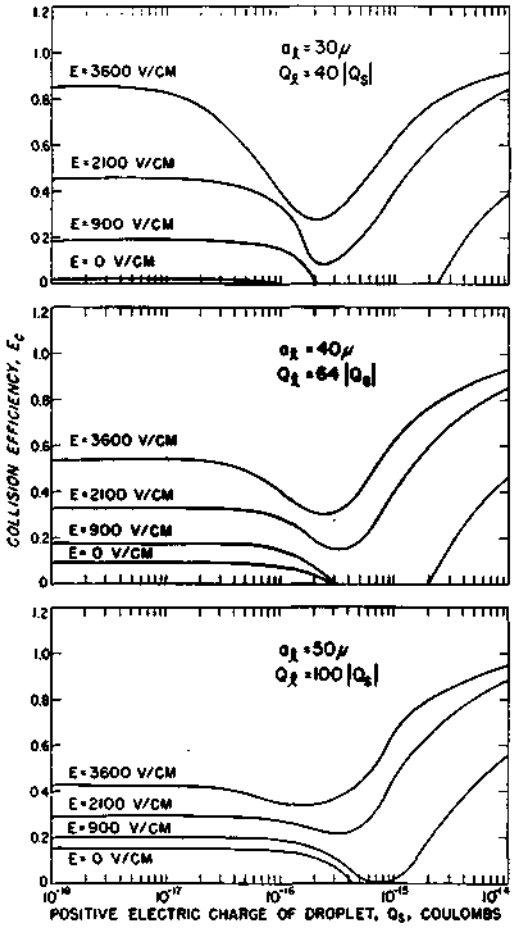

Fig. 5. Collision efficiency curves for a positively charged 5-μ droplet colliding with a 30-, 40-, and 50-μ drop in electric fields oriented at $\beta = 90°$.

sidered in this investigation. *Gunn* [1949], however, observed the charge on raindrops from active thunderclouds to vary approximately as the surface area of the drops. Later, *Gunn* [1954] formulated the problem of the charging of cloud droplets by the diffusion of ions and once again indicated that the charge is proportional to the surface area of the droplets. *Twomey* [1956] measured the charge on individual cloud particles and found the relationship between charge and diameter to be of the form $q = Ad''$, where n has a value between 2 and 3. Therefore, for this work the ratio of the drop-droplet charge magnitudes is taken as the ratio of the surface areas of the pair.

RESULTS

Drop and droplet charged in field-free space. With these two conditions on the magnitude of the charges, the collision efficiencies of 30-, 40-, and 50-μ drops paired with 5- and 10-μ droplets are shown in Figures 1 and 2. As charges of the same sign on a drop-droplet pair increase, their collision efficiencies decrease rapidly to zero because of the additional repulsive electrostatic forces arising between them. The collision efficiencies for a 5-μ droplet (Figure 1) decrease to zero for a charge between 1 and 5 X 10^{-16} coulomb. However, the collision efficiencies do not change appreciably until the charge on the droplet is greater than 1 X 10""

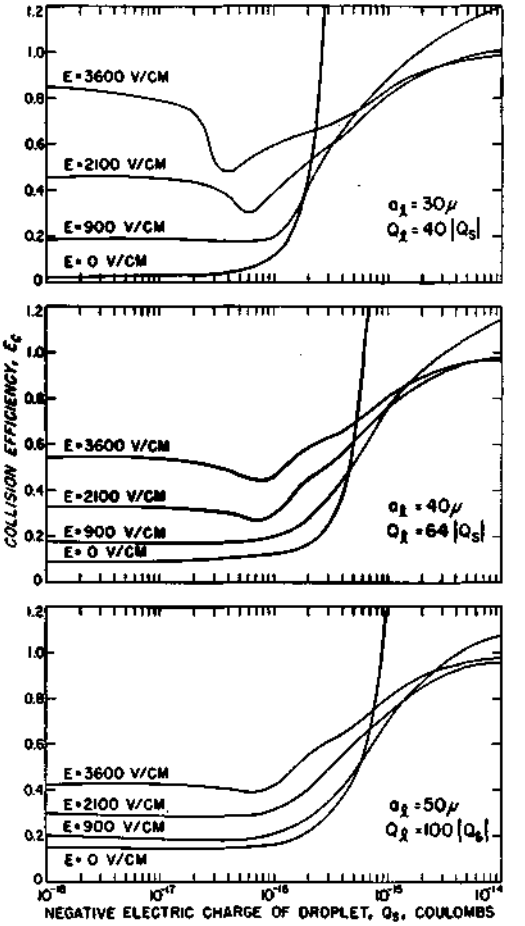

Fig. 6. Collision efficiency curves for a negatively charged 5-μ droplet colliding with a 30-, 40-, and 50-μ drop in electric fields oriented at $\beta = 90°$.

coulomb. The collision efficiencies of the 10-μ droplet are almost constant until the droplet charge exceeds 4 X 10^{-16} coulomb; then the efficiencies decrease to zero for a charge between 2 and 5 X 10^{-15} coulomb.

For drop charges which are of opposite sign to the droplet charge, the collision efficiencies increase as the charges are increased because the electrostatic forces are attractive. There is no appreciable change in the collision efficiencies of the 5-μ droplet until its charge is greater than 1 X 10^{-16} coulomb; then the efficiencies increase rapidly as the charge continues to increase (Figure 2). Although the collision efficiencies for a 10-μ, droplet increase similarly

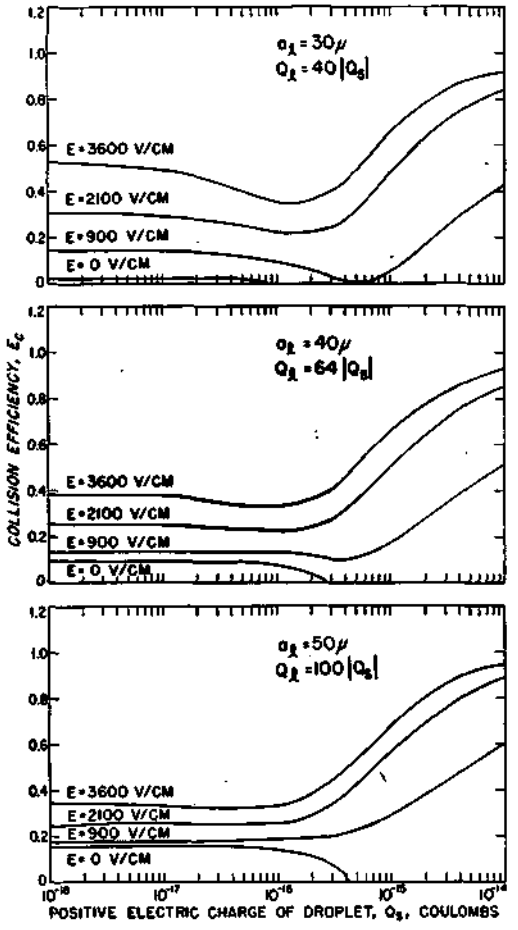

Fig. 7. Collision efficiency curves for a positively charged 5-μ droplet colliding with a 30-, 40-, and 50-μ drop in electric fields oriented at β = 180°.

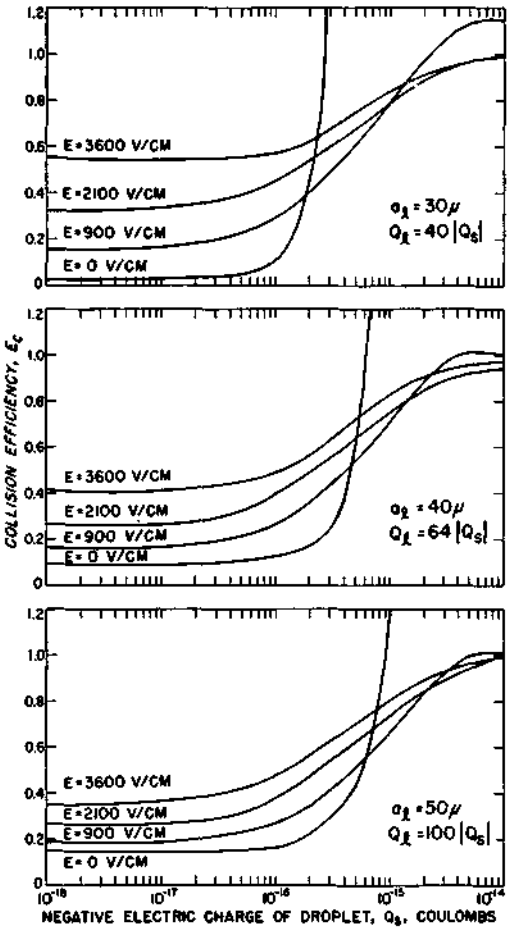

. Fig. 8. Collision efficiency curves for a negatively charged 5-μ droplet colliding with a 30-, 40-, and 50-/4 drop in electric fields oriented at β = 180°.

to those of the 5-μ droplet, the larger droplet requires additional charge before the rapid increase occurs.

Drop and droplet charged in an applied electric field. As in the case of a drop-droplet pair in a field-free region, the sign of charge on the drop is selected to be always positive and the ratio of the charges of the pair is taken to be proportional to the ratio of their areas. By always selecting positive charge on the drop and considering both positive and negative electric fields with a given orientation, we obtain results from all combinations of drop-droplet charges, including negative charge on the drop. For example, with positive charge on both the

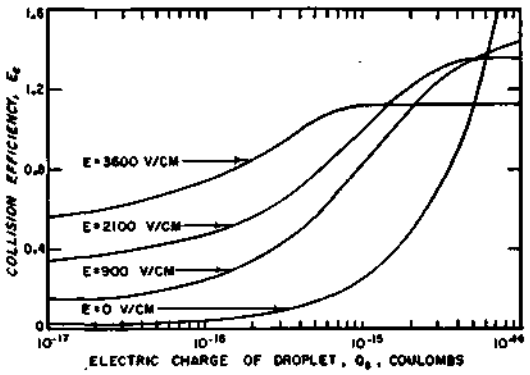

Fig. 9. Collision efficiency curves for a positively charged 5-μ droplet colliding with an uncharged 30-μ drop in electric fields oriented at $\beta = 0°$.

drop and droplet in an electric field oriented at $\beta = 0°$, the results are identical with those obtained with negative charge on both the drop and droplet with an electric field oriented at 180°.

Only electric fields oriented at $\beta = 0°$, 90°, and 180° are considered in this work. It is necessary, therefore, to consider four separate combinations of field orientation and charge sign on the droplet in order to obtain collision efficiencies for vertically applied fields ($\beta = 0°$ and 180°). Because of the symmetry that exists for horizontally applied fields ($\beta = 90°$ and 270°), however, only two distinct combinations of charge sign on the droplet with a field oriented at $\beta = 90°$ need be considered for determining the collision efficiencies.

Figures 3 through 8 show the family of curves of the collision efficiencies of a 5-μ droplet paired with 30-, 40-, and 50-μ drops for various electric fields. These curves indicate that **the** collision efficiencies **are** unaffected **by charge until the droplet charge exceeds 1 X 10"" coulomb. However, the most significant change in the collision efficiencies occurs for an order of magnitude increase in the charge on the droplet.**

In Figure 3 **the** sign of **the** charge **on the** droplet is positive, and **for** no applied field, as discussed previously, the collision efficiencies decrease to zero as the charge increases in magnitude. **For** a greater applied field, however, the efficiencies no longer diminish to zero, but can acquire values greater than unity. **For** additional increases in charge a balance between the electrostatic and gravitational forces is reached, and the computer program becomes unstable. If sufficient charge is placed on the droplet, efficiencies can again be calculated. The values beyond the unstable region increase from zero and approach unity asymptotically. For negative charge on the droplet and no applied field, the efficiencies (Figure 4) increase exponentially as the charge increases. However, in contrast to the no field case, the efficiencies decrease to zero for sufficiently large applied fields and again cause instabilities in the computer program. Further increases in charge beyond the instability region result in efficiencies greater than unity decreasing asymptotically to unity.

Figure 5 shows that the efficiencies decrease as the positive charges increase on the droplet. For the more intense applied fields, however, the efficiency curves reach minimum values, and as the charge continues to increase the collision efficiencies increase. For the less intense fields the efficiencies decrease to zero as in the field-free case. With negative charge on the droplet, the collision efficiencies denoted in Figure 6 do not decrease to zero as the charge increases; instead, the rate of increase of the collision efficiencies is positive but becomes less positive as the electric field is intensified.

For a positive charge on the droplet, the efficiencies, as shown in Figure 7, increase as the charge increases when the larger fields are present. This is a similar result to that obtained for $\beta = 0°$. However, for a negative charge on the

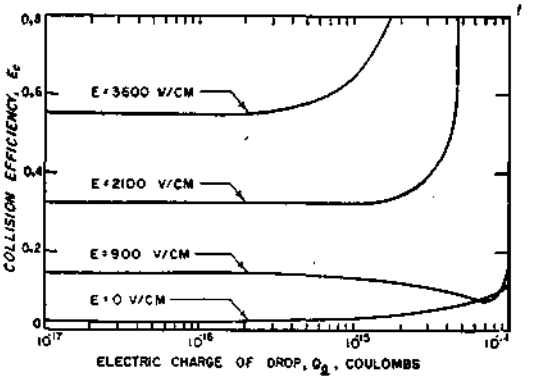

Fig. 10. Collision efficiency curves for an uncharged 5-μ droplet colliding with a positively charged 30-μ drop in electric fields oriented at $\beta = 0°$.

droplet, the efficiencies (Figure 8) also increase as the charge increases. This result is the reverse of that obtained when $\beta = 0°$.

Either drop or droplet charged in an applied electric field. The collision efficiencies of a 30- and 5-μ drop-droplet pair (only one of the pair carrying a charge) in an electric field oriented along the x axis where $\beta = 0°$ are given in Figures 9 and 10. For the 5-μ droplet charged positively, the efficiencies shown in Figure 9 increase as the charge increases, but the curves tend toward a maximum value in excess of unity for appropriate combinations of charge and ambient static fields. The maximum efficiencies reached decrease as the electric field increases. With a positive charge on the 30-μ drop the collision efficiencies (Figure 10) remain almost constant until the charge increases to 2×10^{-16} coulomb. Above this value of charge the efficiencies increase as the magnitude of the charge increases, with the exception of the curve for a field strength of 900 v/cm which decreases slightly before the increase is observed.

SUMMARY AND CONCLUSIONS

These results apply only to drop-droplet pairs which are already charged and are in the presence of an existing electric field. No attempt has been made to explain the origin of the charge or the existence of the electric field. The results show that for small electric fields ($E < 100$ v/cm) the efficiencies of charged droplets in collision with larger drops require several hundred elementary charges on the droplet before measurable effects are calculated for the range of sizes of drop-droplet pairs considered in this report. *Webb and Gunn* [1955] reported observations of the free charge on cloud droplets in nonprecipitating clouds and found the average charge to be of the order of tens of elementary charges. According to the results presented in this paper, charges of this magnitude will not affect the growth of cloud droplets to raindrops.

When the electric field within a cloud exceeds the minimum values suggested by these results and the charges on the individual droplets are in excess of several hundred, the growth of precipitation by a collection process can be materially affected by the changes in collision efficiencies. In a recent paper *Moore et al.* [1964] discussed the importance of charged droplets moving in a very intense electric field after a lightning discharge. The assumption was made in their discussion of the length of the mean free path between collisions that the collision efficiency was unity. This is indeed the shown by the results presented here, when the charges on the droplets exceed approximately 10"" coulomb and the electric field is sufficiently great. It is interesting that this effect is due primarily to the interaction of the charges and the field and is independent of the orientation of the electric field. The cloud droplets can be oppositely charged or of the same sign of charge and the collision efficiencies will still tend toward unity when adequate charges and sufficient field intensities are present.

The study of the growth of precipitation by the collision and coalescence of cloud droplets in the absence of lightning discharges or the extreme fields considered by *Moore et al.* [1964] is complicated by the discontinuous nature of the calculated collision efficiencies. Since there are no reliable measurements of the strength and orientation of electric fields within clouds or any direct observations of the free charge on the cloud droplets, it is difficult to construct a realistic model of an electrified cloud and its charge distribution. It is entirely possible, on the basis of these calculations and results, to have the cloud droplets in one pole of a cloud semirigidly fixed in space by balancing the electrical and gravitational forces. To achieve such a state for the distribution of the various forces does not require extreme fields or charges.

Acknowledgments. This work was supported by National Science Foundation grant NSF-GP-2528. The use of the University of Illinois 7094-1401 computing system was partially supported by National Science Foundation grant NSF-GP-700.

REFERENCES

Fletcher, N. H., *The Physics of Rainclouds,* 386 pp., Cambridge University Press, 1962.

Gunn, R., The free electrical charge on thunderstorm rain and its relation to droplet size, *J. Geophys. Res., 64(1),* 57-63, 1949.

Gunn, R., Diffusion charging of atmospheric droplets by ions, and the resulting combination coefficients, *J. Meteorol, 11* (5), 339-347, 1954.

Krasnogorskaya, N. V., Investigation of collision efficiency of cloud particles, *Proc. Intern. Conf. Cloud Phys. Suppl,* pp. 124-130, Tokyo, 1965.

Lindblad, N. R., and R. G. Semonin, Collision efficiency of cloud droplets in electric fields, *J. Geophys: Res., 68(4),* 1051-1057, 1963.

Moore, C. B., B. Vonnegut, E. A. Vrablik, and D. A. McCaig, Gushes of rain and hail after lightning, *J. Atmospheric Sci., 21* (6), 646-665, 1964.

Nordsieck, A. T., On numerical integration of ordinary differential equations, *Math. Computation, 16(77),* 22-49,1962.

Plumlee, H. R., and R. G. Semonin, Cloud droplet collision efficiency in electric fields, *Tellus, 17(3),* 356-364, 1965.

Sartor, J. D., Some electrostatic cloud-droplet collision efficiencies, *J. Geophys. Res., 65(7),* 1953-57, 1960.

Twomey, S., The electrification of individual cloud droplets, *Tellus, 8(4),* 445-452, 1956.

Webb, W. L., and R. Gunn, The net electrification of natural cloud droplets at the earth's surface, *J. Meteorol., 12(3),* 211-214, 1955.

(Manuscript received January 10, 1966;
revised May 23, 1966.)

THE COALESCENCE DELAY TIME: EFFECTS OF VOLTAGE, VELOCITY, AND HUMIDITY

Richard G. Semonin
Atmospheric Sciences Section
Illinois State Water Survey-

Presented at the 47th Annual Meeting of the
Pacific Division, AAAS with the AMS,
June 13-18, 1966, Seattle

The research reported herein was sponsored by the National Science Foundation through grant NSF GP-2528

THE COALESCENCE DELAY TIMES EFFECTS OF VOLTAGE, VELOCITY, AND HUMIDITY[1,2]

Richard G. Semonin
Atmospheric Sciences Section
Illinois State Water Survey

ABSTRACT

An experiment is described which was designed to examine certain parameters which are considered important in the final stages of the collision-coalescence process.' The voltage between a pair of drops, the relative humidity of the environment, and the impact velocity were studied.

To perform this analysis millimeter size drops were suspended from hypodermic needles and were impacted within a sealed chamber which contained a controlled, but variable, atmosphere. The delay between the time of visual and complete coalescence was determined as a function of the voltage between the drops, the impact velocity, and the relative humidity of the "environment.'

The potential difference between the drops was changed from 0 to 30 volts while the remaining parameters were held invariant. The effects of impact velocity were derived from measurements at approximately 10, 18, and 35 cm/sec. The humidity variations were determined at 10, 50, and 90 percent. In all of the experiments the temperature was maintained at nearly 22°C.

A family of curves of the inverse delay time versus voltage, corresponding to 10, 50, and 90 percent relative humidity, is generated when the velocity Is held constant. The inverse delay time rises sharply and becomes constant at about 0.5 milliseconds^{-1} (2 milliseconds delay time). The constant value is reached when the potential difference between the drops is about 10 volts.

Similar curves are obtained when the relative humidity is fixed and the impact velocity is varied. Again an independence of potential difference is observed near 10 volts. The inverse delay time varies from 0.25 to 1.00 milliseconds"[1] for velocity changes from 10 to 35 cm/sec and greater than 10 volts between the drops.

The implications of such data to the problems of precipitation initiation in warm clouds is briefly discussed.

---

[1]Prepared for presentation at the 47th Annual Meeting of the Pacific Division, AAAS with the AMS, June 13-18, 1966, Seattle.

[2] The research reported herein was sponsored by the National Science Foundation through grant NSF GP-2528.

INTRODUCTION

The efficiency of the coalescence mechanism of rain formation is readily realized when observing tropical clouds. In many areas of the world clouds whose depth is only 2km and whose tops never reach the freezing level can be seen to precipitate. Repeated, almost daily performances of such occurrences annually result in over 8,000 millimeters of rain on the slopes of Mauna Kea on the Island of Hawaii.

Recent evidence substantiates the hypothesis that the coalescence process may also be a very important factor in the formation of rain in mid-latitude clouds. Braham (1965) has reported observations of hydrometeor sizes within cumulus clouds in Missouri which suggest that coalescence between water particles may be of importance in the early development of clouds whose summits are becoming glaciated. We are, therefore, concerned with acquiring comprehensive understanding of the coalescence process in order that the general problem of precipitation initiation and maintenance can be more precisely attacked.

The mere fact that two droplets collide does not mean that they merge together to form a larger particle. The non-coalescence of two droplets is easily demonstrated with a so-called "Rayleigh fountain." A vertically pointed stream of water disintegrates into droplets and through loss of momentum attempt to fall down upon the issuing stream. The result is that the droplets bounce off one another and form an umbrella shaped spray above the fountain. If an electrified rod is brought near the top of the spray the droplets immediately begin to coalesce and the stream soon collapses upon itself due to the rapid coalescence of the droplets.

DELAY OF COALESCENCE OF COLLIDING DROPS

The bounce effect observed by Rayleigh is conceived as due to a thin film of the gaseous medium separating the drops which must be removed before the water surfaces can come into contact. Studies by Lindblad (1964) in our laboratory, following the principles of Prokhorov (1954), have shown that there indeed exists a layer of air between the drop surfaces which deforms the surfaces as the drops approach each other. However, to the unaided eye the drops appear to be in contact. When the drops collide there is an exchange of momentum between them as well as changes in the free energy of the surfaces, even though they are separated, perhaps, by several thousand Angstroms.

The observations suggest that through the gradual elimination of the air from between the surfaces, they come sufficiently close that the final process becomes a matter of random probability. Usually the drop separation decreases to approximately 1000 angstroms and then random perturbations on the surfaces determine the

exact moment of coalescence. Knowledge of the time required to go the distance from visual collision to the 1000 angstroms is requisite to the study of the bounce-off phenomena. Prom these data, it is inferred that a pair of drops must approach each other to within a critical separation and must remain within this distance for a period of time which is dependent upon voltage and impact velocity, before the coalescence can occur.

The coalescence delay time as used in this work is defined as the time interval between the visual collision of the drops and the initiation of the coalescence process. For the large drops used, these times vary from tens of milliseconds down to a few microseconds.

EXPERIMENTAL TECHNIQUE

The drops were formed at the tips of two number-l8 hypodermic needles which were etched so that the tips were relatively flat and sharp. One of the needles was mounted rigidly inside a sealed, electrostatically shielded chamber while the other was mounted on pivots in such a way that the swinging drop would collide with the other without the needles coming into physical contact. The velocity of the swinging drop was varied by changing the arc length through which the pendulum swung. The temperature and relative humidity of the environment within the chamber was measured by means of an electric hygrometer.

A l6-mm Fastax camera was used to take high speed photographs of the profiles of the two colliding drops. This camera can take 16,000 frames per second although most of the data were obtained at 14,000 frames per second.

The potential between the two drops was changed by electrically insulating the two needles and applying variable voltages between them. A Hewlett-Packard vacuum tube voltmeter was used to measure this potential difference. A precision 10 ohm resistor was placed in series with this circuit, as shown in Figure 1. The current in the circuit was monitored by measuring the voltage developed across the resistor with one channel of a dual-beam Tektronix Type 551 oscilloscope. The second channel monitored the relative velocity of the two needles. Both of these variables were recorded by photographing the oscilloscope traces with a Tektronix Type C-12 camera. The oscilloscope was adjusted so that the traces were initiated only with the initial pulse from the photodiode which occurred only when the drops were in visual contact.

The delay time between visual and actual coalescence was determined from the oscilloscope photograph by measuring the interval between the first pulse from the photodlode and the

pulse from the external circuit. The measurements are accurate within 1 percent, A typical sequence of events is shown in Figure 2.

RESULTS

The measurements of the delay time as a function of the potential difference between the drops and the velocity of impact are shown in Figure 3. The inverse of the delay time becomes a constant when the voltage applied between the drops exceeds approximately 10 volts. However, the inverse of the delay time increases rapidly from zero for potential differences between 0 and 10 volts. It is also noted in Figure 3 that the inverse delay time increases with increasing impact velocities. This is more clearly shown in Figure 4. The data shown in Figure 4 indicate that the relationship between the inverse delay time and the impact velocity is linear with the slope of the line dependent on the voltage between the colliding drops. This set of data was acquired in the sealed chamber with an environmental relative humidity of 10 percent and a temperature of about 22°C.

The effects of changing the relative humidity in the chamber, while not as impressive as impact velocity, are shown in Figure 5. Again it is noticed that the inverse delay time increases sharply from zero and becomes constant at approximately 15 volts. The impact velocity for this series of data was 18 cm/sec. These data are again plotted in a different manner in Figure 6. The apparent near independence of the inverse delay time on the relative humidity is shown very clearly in this figure since the slope of the curve relating the inverse delay time with the relative humidity is very small.

DISCUSSION

It would be folly to attempt to relate these results directly to phenomena inside of clouds since there is at least two orders of magnitude difference in the experimental drop sizes and those in clouds. However, it is interesting to speculate on the effects that might be expected if the measurements presented here were strictly applicable to the cloud droplet spectrum.

First, the ambient relative humidity appears to be of little import in the coalescence process. While there is some small effect observed it plays a secondary role compared with other variables investigated. Certainly in the range of humidities that would be expected within clouds the differences in delay times would be entirely insignificant, as seen by inspection of Figure 6.

Secondly, there Is a strong dependence of the delay time upon the voltage between the drops. It has been demonstrated during this experiment that even these large drops will rebound upon impact if the potential difference between them is less than 0.5 volt. This evidence when coupled with observations of a Rayleigh fountain, suggests very strongly that the presence of charge on colliding drops is a necessary ingredient for the coalescence process. The voltage (or charge) is conceived as adding the force necessary to bring the drops more rapidly together across the final critical separation thus permitting the drops' surfaces to come into contact.

Thirdly, the findings on the dependence of the delay time on the velocity are striking. This result is interpreted as again illustrating the necessity for overcoming the critical separation in as short a period of time as possible, that is, while the drops are in contact as defined visually.

The final overall Implication of the data concerns the use of calculated collision efficiencies in modeling clouds and precipitation initiation. In the past calculations by other investigators of the growth of precipitation within clouds by a collision-coalescence mechanism have invoked the assumption of unit coalescence efficiency. The growth of particles was then based strictly on values of the collision efficiency. While it is not possible at the present time to give better values for the coalescence efficiency, evidence is becoming available which shows that the use of the collision efficiencies for such calculations are indeed optimistic.

If the cloud particles are hypothesized to have net zero charge on them, then the collision efficiencies are overestimates of the true collection efficiency due to the neglect of a bounce-off coefficient in the hypothesis. On the other hand, if the assumption is made that the coalescence efficiency is unity, and that the resultant calculations of precipitation growth are consistent with observation, then the data presented in this paper indicate that It must be assumed that the droplets are significantly charged.

REFERENCES

Braham, R. R., "The aerial observation of snow and rain clouds," Proc. Intern. Conf. on Cloud Physics, 492-501, Tokyo, 1965.

Lindblad, N. R., "Effects of relative humidity and electric charge on the coalescence of curved water surfaces," J. Colloid Sci., 19, 729-743, 1964.

Prokhorov, P. S., "The effects of humidity deficit on coagulation processes and the coalescence of liquid drops," Disc. Faraday Soc., No. 18, 41-51, 1954.

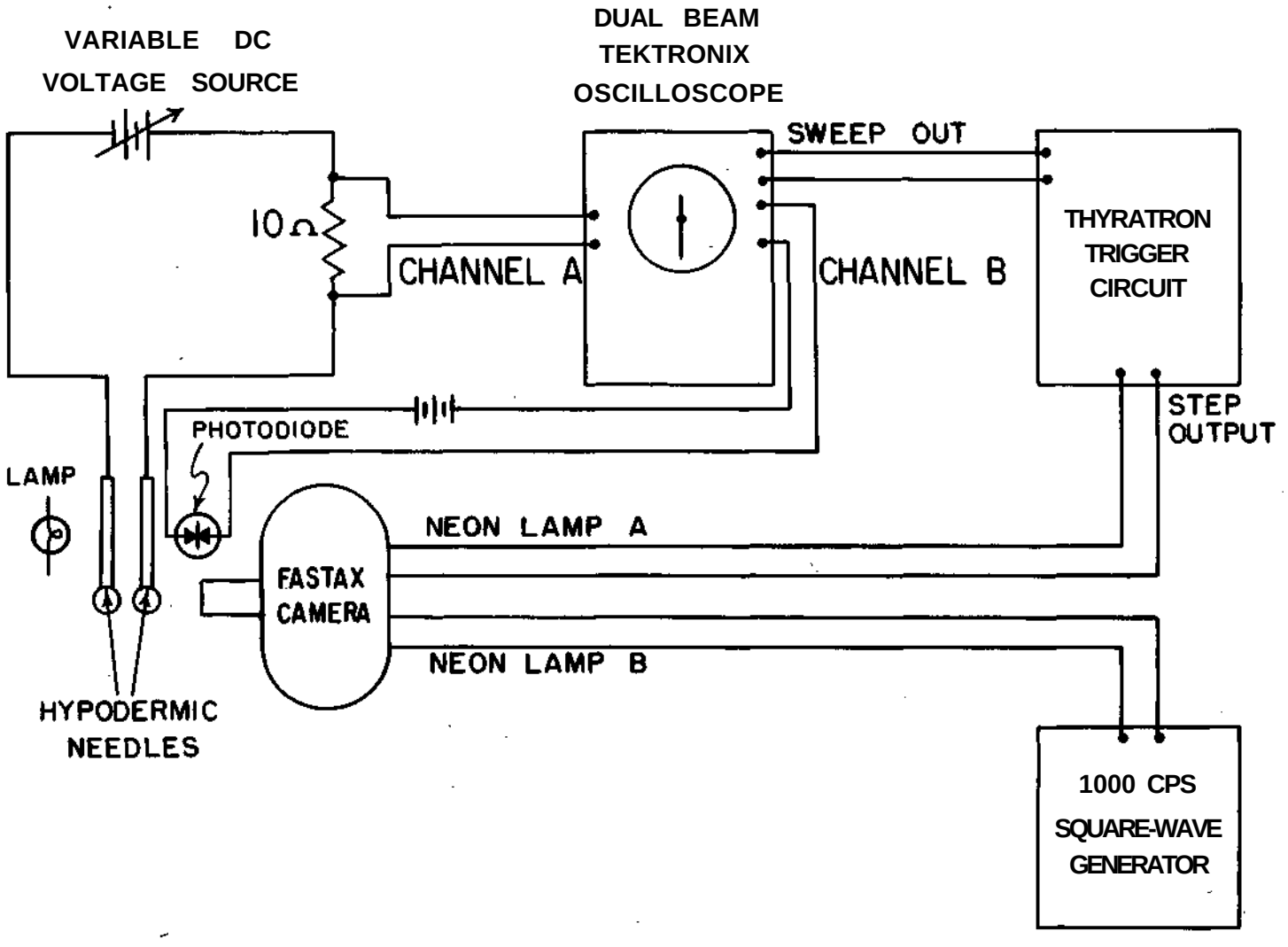

Figure 1. Block diagram of the experimental apparatus used for the determination of coalescence delay time.

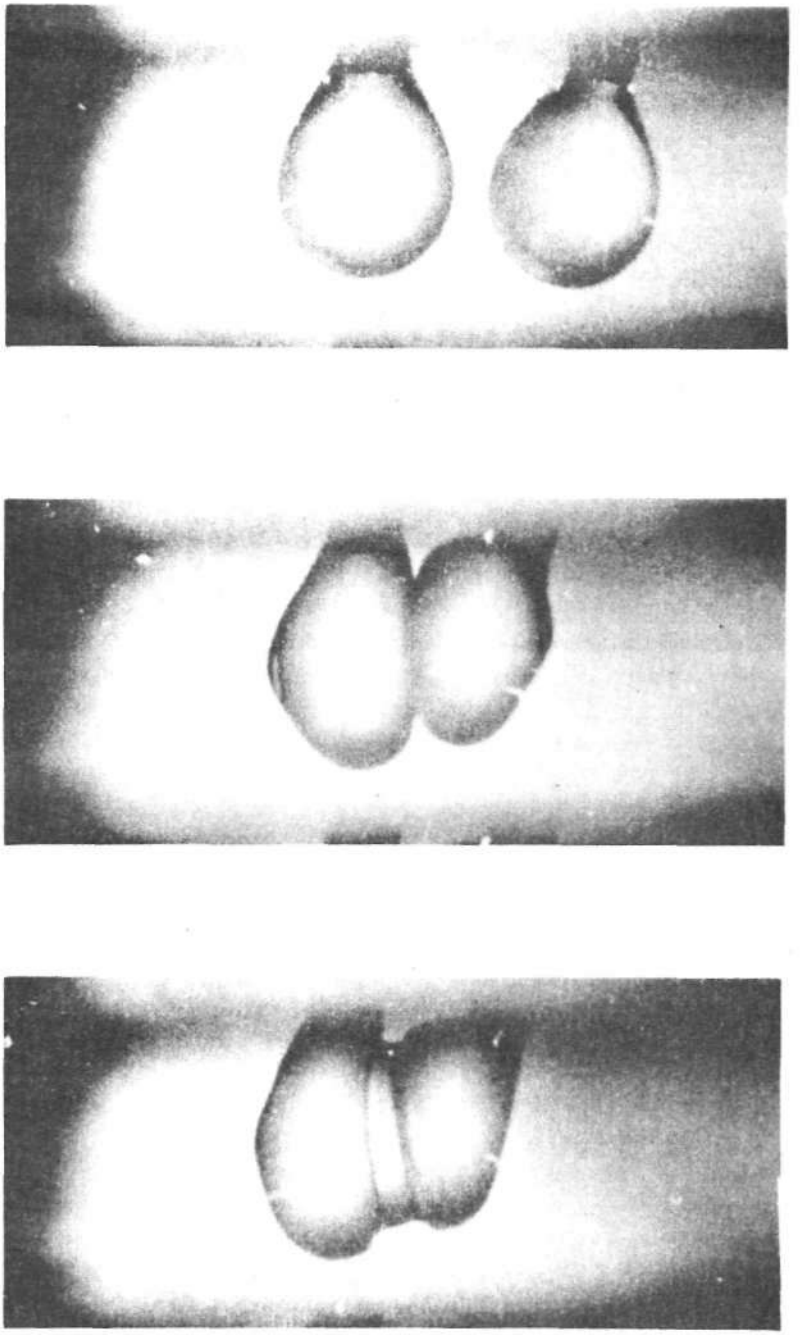

Figure 2. A typical collision and coalescence of a pair of millimeter-size drops.

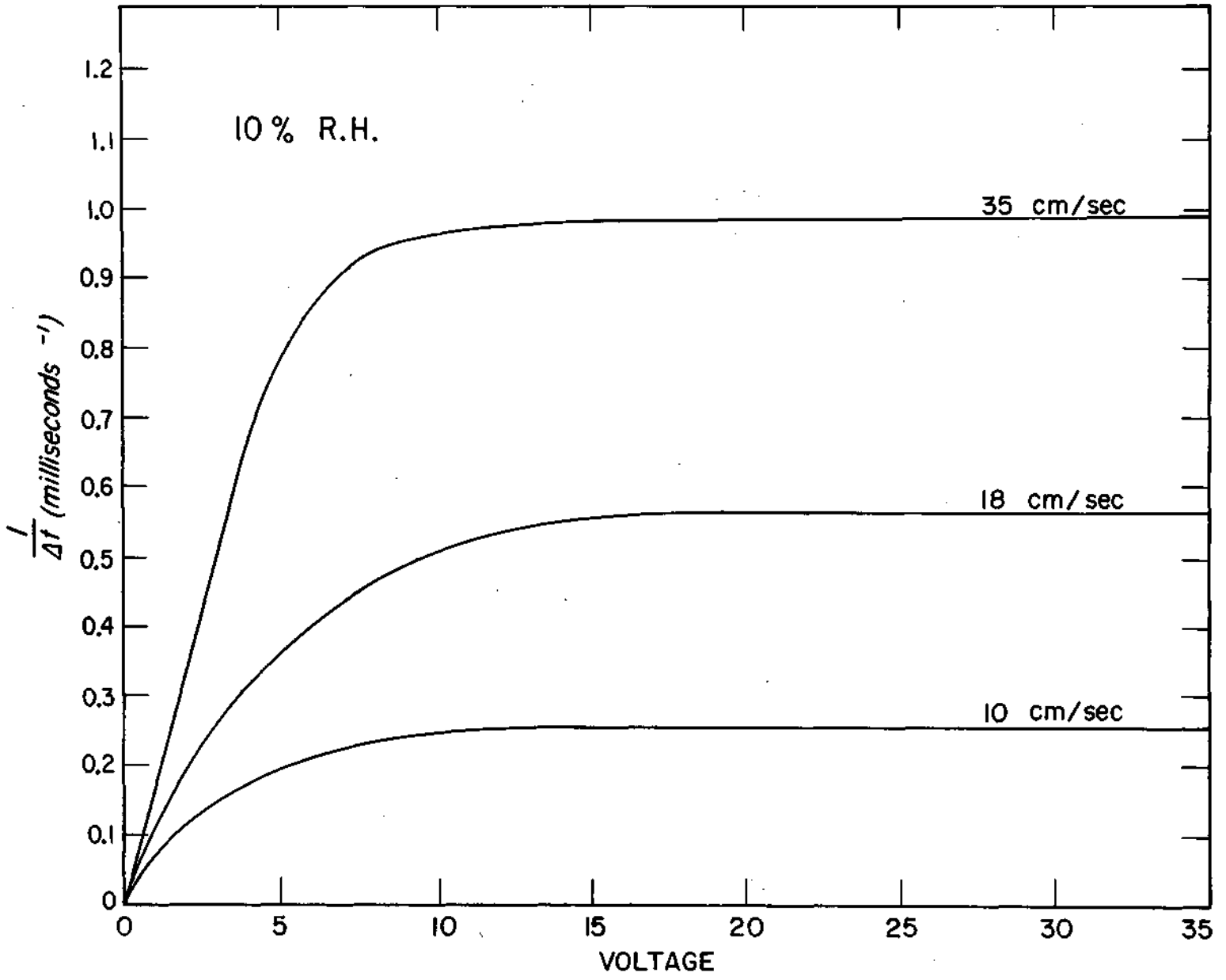

Figure 3. The inverse coalescence delay time versus voltage at impact velocities of 10, 18, and 35 cm/sec and 10 percent relative humidity.

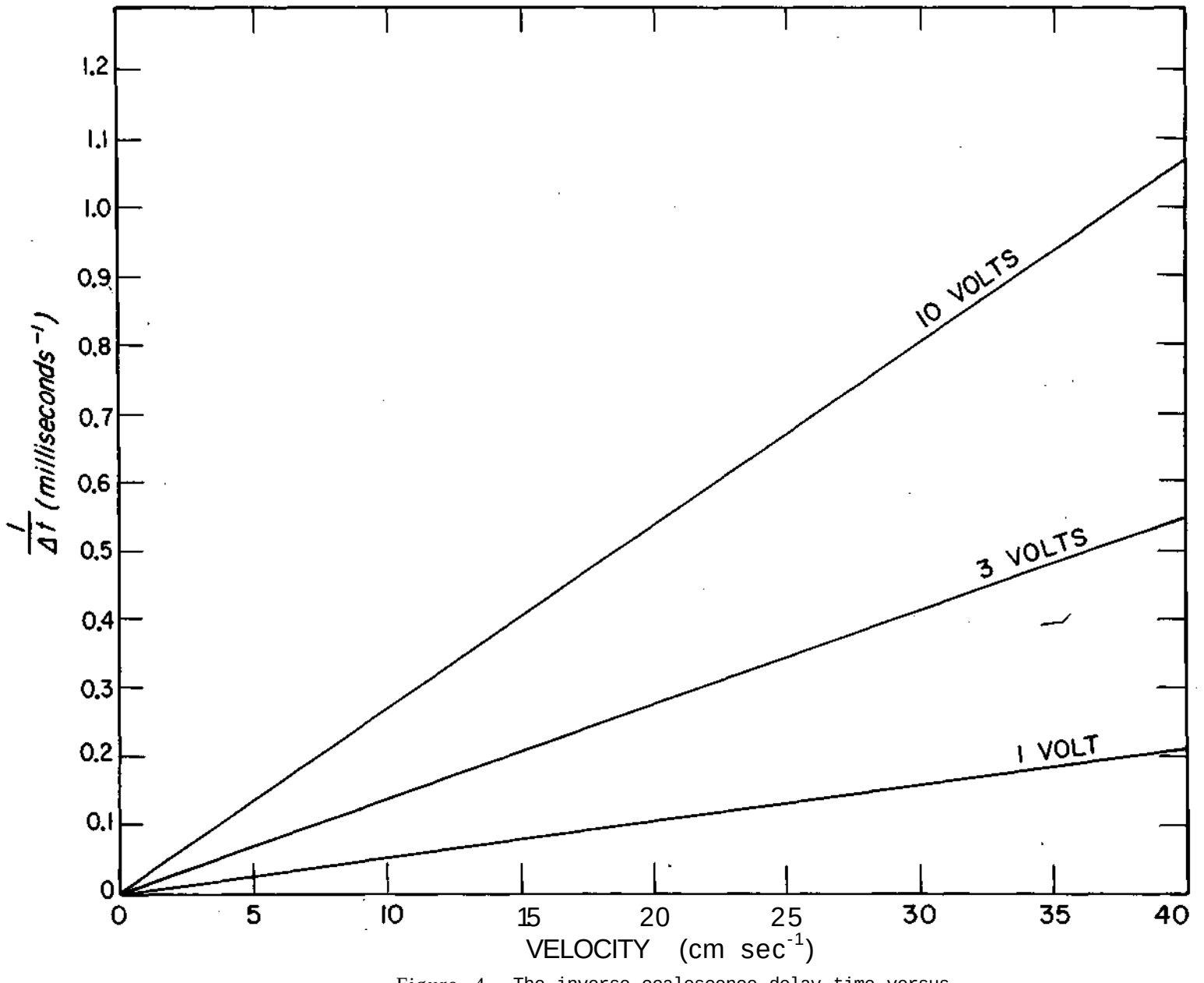

Figure 4. The inverse coalescence delay time versus impact velocity at 1, 3, and 10 volts and 10 percent relative humidity.

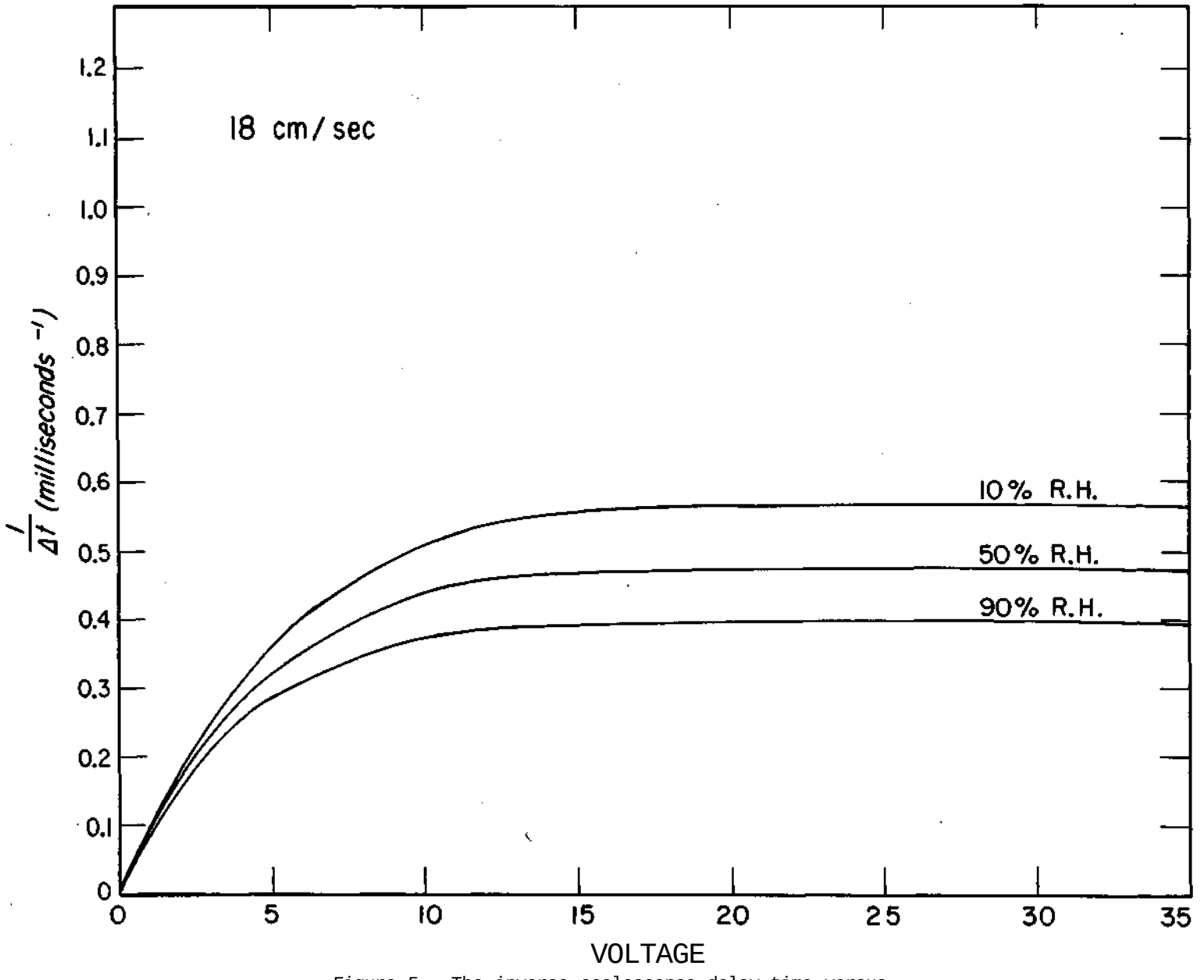

Figure 5. The inverse coalescence delay time versus voltage at relative humidities of 10, 50, and 90 percent and 18 cm/sec impact velocity.

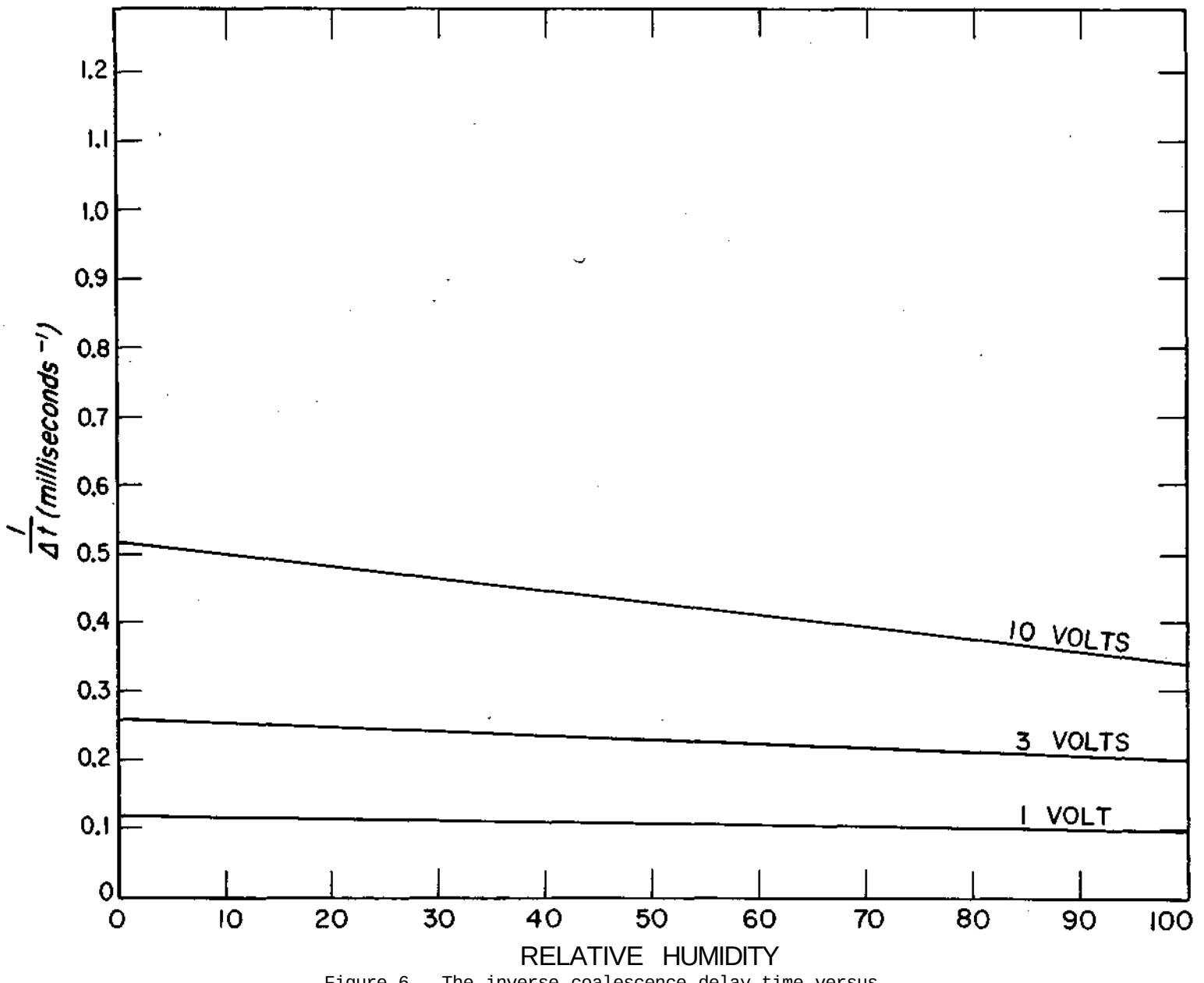

Figure 6. The inverse coalescence delay time versus relative humidity at 1, 3. and 10 volts and 18 cm/sec impact velocity.

Reprinted from the *Journal of Scientific Instruments*, VOL. 42, pp. 635-638, AUGUST 1965

Production of uniform-sized liquid droplets

N. R. LINDBLAD and J. M. SCHNEIDER
Charged Particle Research Laboratory, Illinois State Water Survey, Urbana, U.S.A. and Department of Electrical Engineering, University of Illinois, Urbana, U.S.A.

MS. received 1st April 1965, *in revised form 17th May* 1965

Abstract. A method for producing a stream of uniform-sized liquid droplets and individual droplets is discussed in detail. The method is based on the principle that a cylinder of liquid (jet) is dynamically unstable under the action of surface tension. When a capillary wave of a prescribed wavelength is applied to the jet, the jet will disintegrate into a stream of uniform-sized droplets. Since the droplet size depends on the capillary tube through which the liquid flows, the size can be easily varied. A piezoelectric transducer is used to produce the capillary wave on the jet. The apparatus discussed will produce droplets in a range between 25 and 350 μm in radius. The method is unique in that the droplet size can be precisely controlled and individual droplets can be produced at will.

1. Introduction

To study the collision and coalescence of water droplets in the cloud droplet range requires a device capable of producing uniform-sized droplets. A number of such devices now exist (Dimrock 1950, Freier 1960, Mason *et al.* 1963, Ryley and Wood 1963). A method has been proposed by Mason (1964) to produce individual droplets as well. This paper presents a different device that precisely controls droplet size and produces either a stream of droplets or individual droplets at will. Theoretical bases for the device are provided, and the apparatus and its operation are described.

The device described here is a further sophistication of one proposed by Schneider and Hendricks (1964). Its operation is based on the distintegration of a cylinder of liquid (jet) caused by a capillary wave or disturbance applied to the jet which makes it dynamically unstable under the action of surface tension. The theory of jet disintegration into droplets was investigated by Rayleigh (1879). For this device the disturbance on the jet was produced by electromechanically exciting the capillary tip into longitudinal oscillations which are used to perturb the jet of liquid. A stream of droplets or an individual droplet can be formed in the range 25-350 μm in radius. The size of the droplet can be varied by changing the inside diameter of the capillary tube. Thus, droplets larger or smaller than those discussed in this paper can be made. -

2. Droplet production theory

When a jet of radius a is formed from a capillary tube of radius r_0 the jet eventually disrupts into a series of small droplets random in size, This phenomenon occurs because the jet is dynamically unstable under the action of surface tension. Rayleigh (1879) showed that whenever the wavelength of the disturbance on the jet is greater than the circumference of the jet, surface tension tends to produce instability. He also showed, from the energy standpoint, that the most rapid instability of a jet occurs when the wavelength of the disturbance λ_m is 9.016 a. This wavelength is the most desirable for the production of uniform-sized droplets.

A primary consideration in forming a jet of liquid from a capillary is the determination of the average velocity of the liquid in the capillary tube that is necessary to form the jet. This can be obtained from an energy balance equation for a jet issuing from a capillary tube. The rate of energy flow into the jet from the capillary tube is given by $dE_1/dt = \frac{1}{2}mv_1^2$, where v_1 is the velocity of the liquid in the capillary tube, p is the liquid density and $m = prra^2v_1$. The conservation of energy requires that dE_t/dt must be equal to the sum of the rate of flow of kinetic energy dE_2/dt across any plane perpendicular to the jet and the rate of increase of surface energy dP_2/dt which is the result of the constant formation of new jet surface. Since the average jet velocity v_2 is assumed constant, $dE_2/dt = \frac{1}{2}\, mv_2^2$. Also, $dP_2/dt = 2av_2T$, where $2vav_2$ is the rate at which new surface is formed and $T$is the surface tension. Thus, the energy balance equation is

$$\frac{dE_1}{dt} = \frac{dE_2}{dt} + \frac{dP_2}{dt}. \tag{1}$$

In order to form a jet of liquid at the end of a capillary tube the term dE_1/dt must be greater than the amount of energy per unit time required to create the jet surface. Thus

$$\frac{dE_1}{dt} > \frac{dP_2}{dt}$$

or

$$\tfrac{1}{2}\, \dot{m}v_1^2 > 2\, \pi av_2T.$$

By solving the latter inequality for v_1, using $\dot{m} = \rho\pi a^2v_1$ and assuming $v_1 = v_2$ one can obtain the minimum average velocity in the capillary tube necessary to form a jet, namely,

$$v_1 > 2\left(\frac{T}{a\rho}\right)^{1/2}. \tag{2}$$

Equation (2) is plotted in figure 1 for a number of jet diameters A. Since tube manufacturing companies usually give the inside and outside diameters in terms of mils, it is convenient to retain these units. Our experimentally determined relationship between the jet diameter and the inside diameter of the capillary tube was approximately $A = 0.8D$; however, Harmon (1955) gave a theoretical value of 0.866 for this ratio. Our empirical relationship was determined by using electrochemically etched capillary tips, but it may change with differences in capillary tip geometry. This equation (2) was used to plot, in figure 1, the minimum

velocity boundary of the forbidden region of operation with water. For instance, for A = 6 mils the minimum average velocity of the liquid in the capillary tube is 194 cm sec^{-1}. For velocities less than 194 cm sec^{-1} a jet will not form at

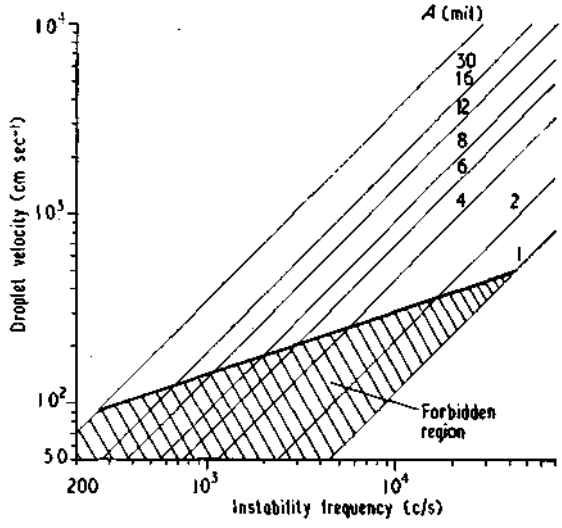

Figure 1. Droplet velocity plotted against instability frequency for various jet diameters.

the end of the capillary tube. Thus, velocities larger than 194 cm sec^{-1} are necessary to form a jet. Equation (2) has been experimentally verified for a number of capillary tubes by Schneider (1964 Ph.D. Thesis, University of Illinois).

The frequency for the most rapid instability is given in figure 1 as a function of jet velocity (droplet velocity) for various jet diameters. An electromechanical transducer was used to transmit mechanical vibrations to the capillary, and thence to the jet. The approximate frequency f for the voltage to be applied to the transducer can be determined from the wave equation

$$f = \frac{v_2}{\lambda_m} \tag{10}$$

where v_2 is the velocity of the jet.

When the jet has been disturbed and A is the wavelength of a given undulation, then the mass M of the undulation (Schneider 1964 Ph.D. Thesis, University of Illinois) is

$$M = \pi a^2 \rho \lambda. \tag{3}$$

The mass given in (3) is equal to the mass of a droplet of radius r since each undulation ultimately becomes one droplet. Hence

$$r = \left(3a^2 \frac{\lambda}{4}\right)^{1/3}. \tag{4}$$

Substituting for A that wavelength λ_m, which produces the most rapid instability the droplet radius is given by

$$r = 0{\cdot}945\, A \tag{5}$$

where A is the jet diameter. Equation (5) can be written in terms of the inside tube diameter D if the coefficient of contraction is known. The theoretical plot of equation (5) is shown in figure 2, and data points are shown as circles.

The radius of the individual droplets of a uniform stream is determined. by measuring the mass flow rate of the liquid through the capillary and dividing by the frequency of excitation of the transducer. Since one droplet is formed for each cycle of the transducer drive frequency this yields the mass of each droplet and hence the radius of each droplet. Since the mass flow rate can be measured very accurately with a pan balance and the frequency can be measured very accurately with a frequency counter, the mass of each droplet

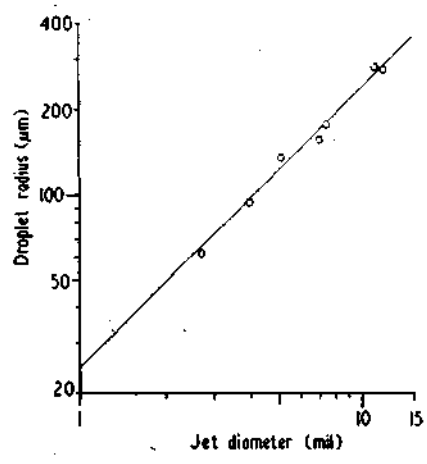

Figure 2. Jet diameter plotted against resulting droplet radius.

can be measured with great precision. The overall error in the determination of droplet radius is of the order of ⅓%. The variance between droplet radii must be within this tolerance because no size variation can be measured even under high magnification (50 x).

It should be indicated in passing that the wavelength A can also control the size of the droplets. However this effect is small since (4) shows that the radius of the droplet is proportional to $A^{1/3}$. Moreover, A must lie in the range between seven A and fourteen A for stable synchronization of droplets (Schneider 1964 Ph.D. Thesis, University of Illinois).

The minimum velocity necessary to form a jet has been calculated from an energy consideration. The pressure necessary to obtain such a velocity in a capillary tube of length / and radius a can be calculated from the Poiseuille equation

$$Q = \frac{\pi a^4}{8\mu l}(P_1 - P_2). \tag{6}$$

where Q is the volume flow rate through the capillary tube, μ is the dynamic viscosity, and P\ and P_2 are the values of the mean pressure at the two ends of the tube. In terms of the average velocity (over the cross section of the capillary tube), the volume flow rate can be written as

$$Q = \pi a^2 v_1. \tag{7}$$

Assuming $P_1 > P_2$ in (6) and equating the two values of Q, the pressure necessary to obtain a velocity v_1 is

$$P_1 = \frac{8\mu l v_1}{a^2}. \tag{8}$$

Substituting into (8) the value of μ for water and the value a = ½A, and multiplying by 1.45 x 10^{-5} to change the units to lb in^{-2}, we have

$$P_1 = 46{\cdot}6 \times 10^{-7}\, \frac{l v_1}{A^2}. \tag{9}$$

Thus, equation (9) gives the approximate pressure required to form a jet of diameter A. The actual pressure used would be a few pounds per square inch higher because the minimum velocity necessary to form a jet was used in the calculation. Since P_1 is inversely proportional to A^2, very high pressures are required for the small capillary tubing. This can be somewhat compensated for in that, since P_1 is proportional to l, shorter tubes can be used for the smaller diameters.

Droplets smaller than 25 μm can be formed when the instability frequency differs slightly from the theoretical value. In this case, two droplets are formed at the tip of the jet, one being approximately the predicted size and the other being a very small satellite drop. Because satellite droplets spray out at an angle with respect to the capillary tube, they are easily separated from the main stream of droplets. Thus, these satellite droplets can be used as the droplets of primary interest.

3. Experimental apparatus and its operation

The discussion of the experimental' apparatus has been divided into two sections, mechanical and electrical. The first section has to do with the mounting of the transducer and the etching of the capillary tubes. The necessary electronics, such as the amplifier used to produce the voltage for the transducer, and the pulse generator used on the charging electrode, are discussed in the electrical section.

3.1. *Mechanical apparatus*

A 'PZT bimorph' transducer mounted as a cantilever was used to produce the mechanical vibrations on the capillary tube. The transducer was 1 in. long, 0.0625 in. wide and 0.024 in. thick. The transducer mounting is shown in figure 3. The capillary tube was made of stainless steel.

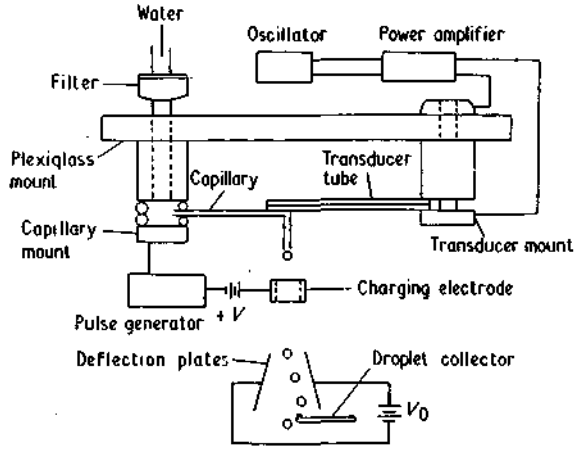

Figure 3. Schematic diagram of the experimental apparatus.

The pressure used to force the water through the capillary tube was obtained by means of a nitrogen tank with a calibrated regulating valve. The water was filtered with a Millipore filter (pore size 0.8 μm) to prevent clogging the small capillaries.

The capillary tips were etched to remove irregularities. The solution found most effective in etching the capillary tips was the following: 25 g of chromium trioxide, 133 ml. of. glacial acetic acid, and 7 ml. of distilled water. The capillary tips were etched three times. During the first etching the apparatus was operated at approximately 10 mA and during the second and third etching at approximately 5 mA. These numbers apply to tubing with an inside diameter of 6 mils. For smaller capillary tubes correspondingly smaller values of current should be used so that the current density at the tip is approximately the same as for the 6 mil tube. This procedure left the capillary tip with only a few very small irregularities.

3.2. *Electrical apparatus*

The transducer electrodes were made of silver fused to the ceramic. When an a.c. voltage was applied to the silver faces of the transudcer, it vibrated in a manner similar to that of a cantilever beam. Since the capillary tube was glued to the free end of the transducer, the vibrations were transmitted to the capillary. The PZT bimorph is virtually independent of temperature and can be operated at low a.c. voltages (30-100 v peak to peak) which are two important advantages over the normal barium titanate transducer. For the purpose, of droplet production, the barium titanate could not be operated at resonance and therefore high a.c. voltages (of the order of 1000 v peak to peak) were required to produce sufficient mechanical excitation. At this high voltage the transducer tended to heat which reduced its mechanical ouput. Thus, to maintain the appropriate mechanical output the transducer must be cooled. The bimorph circumvented these problems. In fact, the small capillaries with inside diameters from 1 mil to about 10 mil can be excited with a simple audio generator with a maximum peak output voltage of 40 v. For larger capillaries, the oscillator signal should be amplified to yield a peak to peak applied voltage of approximately 80 v which should be sufficient for even the very large capillaries.

The main components in the electrical apparatus are shown in a block diagram in figure 3. The desired signal from the oscillator was fed into the power amplifier which excited the transducer.

In normal operation a stream' of droplets of uniform size, equally spaced, was produced. To form a stream of charged droplets a cylindrical charging electrode was placed beneath the capillary tip and coaxial with it. A potential difference applied between the charging electrode and the capillary tube produced a stream of uniformly charged droplets. By placing downstream a pair of deflection plates to which an electrical potential difference is applied, the charged droplets are deflected.

Individual droplets can be formed by pulsing the charging electrode with a voltage equal to $-V$ to cancel the $+V$ of the battery shown in figure 3. The time interval of the pulse voltage should be slightly less than the period of the transducer frequency. This creates a single droplet which is uncharged. The number of individual droplets desired can be obtained simply by adjusting the pulse repetition rate. Obviously, the formation of single droplets depends on the fact that the voltage pulse occurs concurrently with the formation of a droplet, or synchronically with the transducer drive frequency.

Figure 4 shows a 120 μm charged droplet pulsed out of an uncharged stream of droplets. Once the droplet is pulsed out of the main stream, aerodynamic forces rapidly slow the droplet down. This is indicated by its position with respect to the main stream, i.e. the droplet originally following the droplet pulsed out is now nearly even with it. In the example shown one out of 49 droplets was being pulsed out of the main stream.

The droplets were observed with light from an electronic stroboscope. To synchronize the light flashes with the

droplets, the signal from the amplifier was fed into an oscilloscope. The sweep frequency was set so that approximately 6 cycles of the input signal were displayed. The square pulse from the scope 'gate out' was then used to fire the Strobotac, which illuminated every sixth droplet.

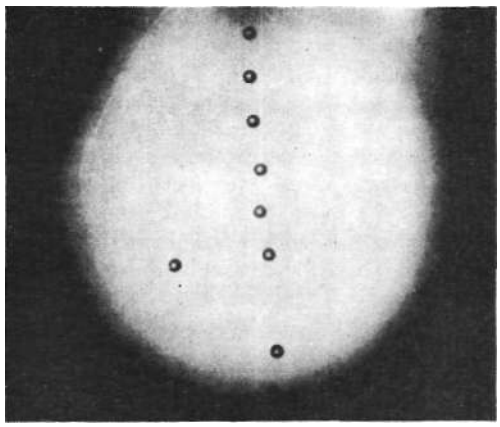

Figure 4. A charged droplet pulsed out of a stream of uncharged droplets.

One of the simplest ways to measure the electric charge on each droplet of a uniform stream of droplets is by determing their deflection in a uniform electric field. If the stream of droplets enters the uniform field at a high velocity the effect of air resistance can be neglected. The deflection caused by the electric field is given by $x = (q/2M)Et^2$, where q is the charge on the droplet, M the mass of the droplct, E the electric field intensity, and t is the time the droplets have been in the field. The method described by Hendricks (1962) can be used to measure the charge and velocity of a single droplet. However, the smallest charge that can be measured with this method is on the order of 10^{-16} coulomb.

4. Concluding remarks

The apparatus described herein to produce a stream of uniform droplets is simple and inexpensive to build. To generate single droplets requires more extensive electronic equipment, such as a pulse generator and power supply for separating an uncharged droplet out of a stream of charged droplets. The method is unique in that uncharged or charged droplets can be produced at will in the range from 25 to 350 μm in radius.

The apparatus has a number of applications in various fields of research where droplets are needed. For example, in studying the collision and coalescence of cloud droplets two such devices could be situated at any desired orientation for observation of collisions.

Acknowledgments

The authors wish to thank Professor C. D. Hendricks, Professor of Electrical Engineering, and Mr. R. G. Semonin, Associate Meteorologist, Illinois State Water Survey, for their criticism and helpful suggestions. This work was supported by grants NSF GP-2528 and AFOSR-107-64.

References

DIMMOCK, N. A., 1950, *Nature, Lond.*, **166,** 686-7.

FREIER, G., 1960, *J. Geophys. Res.*, **65,** 3979-85.

HARMON, D. B., 1955, *J. Franklin Inst.*, **259,** 519-22.

HENDRICKS, C. D., 1962, *J. Colloid Sci.*, 17, 249-59.

MASON, B. J., BROWNSCOMBE, J. L., 1964, *J. Sci. Instrum.*, 41, 258.

MASON, B. J., JAYARATNE, O. W., and WOODS, J. D., 1963, *J. Sci. Instrum.*, 40, 247-9.

RAYLEIGH, LORD, 1879, *Proc. Lond. Math. Soc*, 10, 4-13.

RYLEY, D. J., and WOOD, M. R., 1963, *J. Sci. Instrum.*, 40, 303-5.

SCHNEIDER, J. M., and HENDRICKS, C. D., 1964, *Rev. Sci. Instrum.*, 35, 1349-50.

UNWIN BROTHERS LIMITED, WOKING AND LONDON (B4498)

Reprinted from JOURNAL OF COLLOID SCIENCE, Volume 20, No. 6, August 1965

JOURNAL OP COLLOID SCIENCE 20, 610-616 (1965)

AN APPARATUS TO STUDY THE COLLISION AND COALESCENCE OF LIQUID AEROSOLS[1]

J. M. Schneider, N. R. Lindblad, and C. D. Hendricks

The Charged Particle Research Laboratory, Department of Electrical Engineering, University of Illinois, and the Illinois State Water Survey, Urbana, Illinois

Received February 8, 1965

ABSTRACT

An apparatus used to study collision and coalescence of liquid aerosols and some of the physical quantities enhancing or hindering these processes is described. The relative trajectories, collision, and coalescence of two oppositely charged water droplets are shown for the droplets approaching at right angles. The droplets were 96 μ and 79 μ in radius and had velocities at impact of 330 cm./sec. and 110 cm./sec, respectively. It was found extremely difficult to make the two droplets collide when both were highly charged with the same sign of charge. However, droplets highly charged with the opposite sign of charge had a high collision rate.

INTRODUCTION

Some of the factors which enhance or hinder the coalescence or noncoalescence of liquid droplets have been studied extensively by methods which mechanically constrain the droplets (1-4). The methods used by Berg (1) and Plumlee (2) are essentially the same. In their experiment, the two droplets were supported on two wires or capillary tubes, one of which was movable while the other was held stationary. The droplet on the movable wire was made to collide with the stationary droplet and the collision was photographed. Prokhorov (3) and Lindblad (4) studied the coalescence process of two curved liquid surfaces by microphotography of the interference patterns produced as the two surfaces moved together while illuminated with monochromatic light. In these two experiments half-drops were supported and formed on the ends of two capillary tubes mounted vertically one above the other.

Our experiment differed significantly from the experiments described above in that the droplets were not mechanically constrained. This was a big advantage, since one of the principal objections to the earlier work was that the forces of constraint could drastically change the coalescence process. Moreover, the size of our droplets simulated much more closely the sizes of droplets found in fogs, rain clouds, and other aerosols of common interest.

[1] This work was supported in part by AFOSR Grant 107-64 and in part by NSF Grant GP 2528.

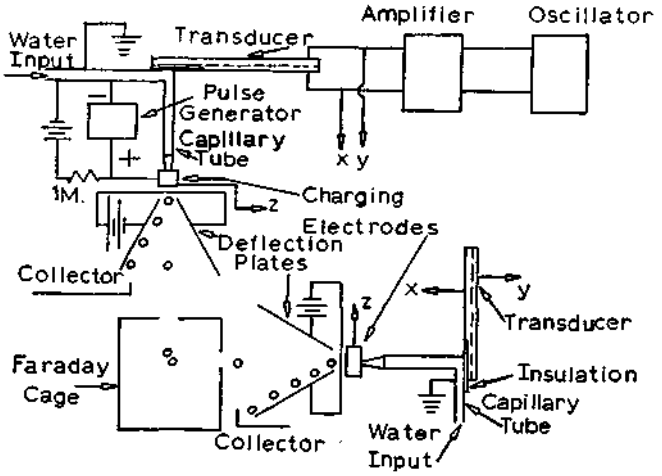

FIG. 1. Schematic diagram of experimental apparatus to study the collision of two liquid droplets.

THE EXPERIMENTAL APPARATUS AND ITS OPERATION

The method of production of a stream of uniform-sized droplets equally spaced, and the extension of this method for production of single droplets of known size, has been reported by Schneider and Hendricks (5) and in more detail by Lindblad and Schneider (6).

The uniform droplets are formed by launching a disturbance (capillary wave) of a prescribed wavelength onto a jet of liquid. This disturbance when properly adjusted causes the jet to disintegrate into a stream of uniform-sized droplets. Since the droplet size depends on the inside diameter of the capillary tube, the size can be varied easily by changing capillary tubes. The apparatus actually used in the experiment is illustrated diagrammatically in Fig. 1.

The capillary tube is vibrated at the desired frequency with the piezoelectric transducer, and this vibration causes a capillary wave to be launched on the jet. As the droplets are formed they can be charged by applying a potential difference between the charging electrode and the capillary tube. When charged droplets enter the region between the deflecting plates, they are deflected toward the collector that is placed downstream below the plates.

Single droplets can be separated from the main stream by applying to the charging electrodes a pulse of voltage that exists during the time of formation of a droplet. Since this one droplet will then have a different charge from the others, it will undergo a different deflection in the region of the deflecting field. The charge on the droplet "pulsed out" of the main stream is determined by the relative amplitudes of the d.c. and pulse voltages on

the charging electrode. Thus, the charge on the droplet can be controlled by simply adjusting the amplitude of the applied pulse.

The method used to determine the radius of the droplets was to measure the mass flow rate through the capillary, and the frequency of excitation of the transducer. Because one droplet is produced for each cycle of the transducer frequency, the ratio of the two measured quantities yields the mass of a single droplet. Since the mass flow rate can be measured with great precision using a pan balance and the frequency can be determined very accurately with a frequency counter, the mass of a droplet can be measured with great overall accuracy (much less than one percent). No size variation among droplets can be observed even under high magnification (50 X).

In the present experiment two droplets were produced by operating two such devices at right angles, as shown in Fig. 1. One droplet generator was mounted on a three-dimensional micromanipulator so that the trajectories of the droplets produced by it could be controlled and collision obtained. The two droplets collided in a Faraday cage which was protected from the ambient air currents by a Plexiglas box. The size of the cage was approximately 20 X 20 X 30 cm^3. The two droplet generators were also enclosed to protect them from external air currents. In the cage the charge and velocity of the two droplets were measured before collision. The droplets were illuminated with a Strobotac flash unit and photographed with a 4 X 5 camera. The vertical and horizontal distances from the collision region to the charging electrodes were approximately 16 cm. The two droplets were pulsed out of the stream and into the cage at the rate of 10 droplets per second. This rate allowed only one vertical and one horizontal droplet to be in the Faraday cage at a given time. Hence, the hydrodynamic forces on the droplets were not affected *by* any extraneous disturbances.

This involved tremendous ballistics problems, and the utmost care was necessary in colliding 100 μ droplets 16 cm. from their point of generation. As an example, it was found that 100 mv. of 60 cycle hum on a 100 v. peak-to-peak transducer drive supply was sufficient to cause intolerable jitter in the droplet trajectories. Thus, all supply voltages had to be extremely pure signals. However, after such idiosyncrasies were isolated, the experiment proceeded with little difficulty.

A diagram of the electrical apparatus is shown in Fig. 2. The signal from the oscillator was fed into the amplifier, where it was amplified so that sufficient voltage was available for the transducer. Since it was very difficult to construct two identical droplet generators because of differences in transducers, capillary tubes, etc., it was necessary to feed the signal from the amplifier into two final amplitude adjustments and a phase shifter. These were used to make the final stability adjustments on the two droplets pulsed out of the main streams. The oscillator signal was also fed into an

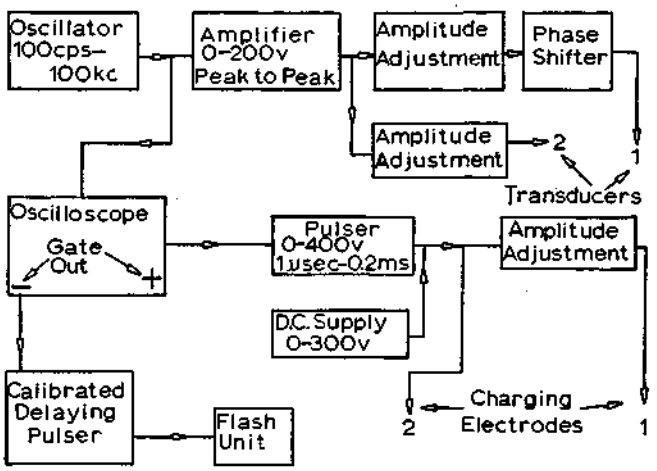

FIG. 2. Block diagram of the electrical apparatus.

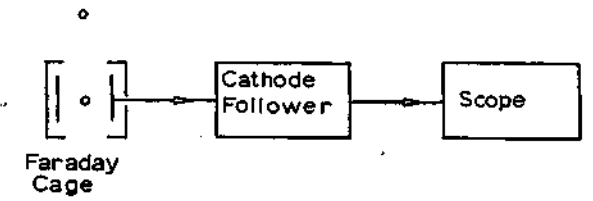

FIG. 3. Schematic diagram of electrical apparatus to measure the charge on the droplets.

oscilloscope used for triggering the charging electrode pulser and into a calibrated delaying pulser used for triggering the Strobotac. The pulser produced a variable-amplitude negative pulse that was applied to the charging electrode to pulse the two droplets out of the stream. Again, because of the differences between the two droplet generators, it was necessary to have a variable-amplitude adjustment on the pulse amplitude for one of the electrodes. Not shown in Fig. 2 is a pulse inverter that was used to produce droplets with opposite charge. The d.c. power supply shown in the figure applied a steady potential between the charging electrode and the capillary tube. This steady potential was used to bias the stream of droplets, that is, by varying the steady voltage on the charging electrode the main stream of droplets could be deflected to any convenient position. Also, as was previously mentioned, the relative amplitudes of the d.c. and pulse voltages determined the charge on the drops pulsed out. The calibrated delaying pulser acted as a trigger for the flash unit so that the droplets could be observed and photographed at any convenient location.

Figure 3 is a diagrammatic representation of a Faraday cage charge

detector that measured the charge and velocity of the single droplets just after they entered the large Faraday cage. The Faraday cage charge detector consists of two electrodes electrically insulated from one another. When a charged droplet passes through the inner electrode, an approximately equal and opposite charge is induced on the inner electrode. Thus, because of the capacitance between the inner electrode and the outer electrode, a potential difference is induced between them. If this potential difference is amplified and displayed on a scope, the trace can yield the charge and velocity of the droplet.[2] The inner conductor of our Faraday cage charge detector was 5 mm. in diameter and 1.08 cm. in height. With the calibrated delaying pulser the average collision velocity of the droplets could be determined at any point in the large Faraday cage. The smallest charge that could be measured on the droplets was approximately 1000 electrons. It was necessary to keep the charge detector inside the large cage to shield it from all external equipment and electrical sources.

RESULTS

In Fig. 4 the pulse from a negatively charged vertical droplet is shown as it passes through the Faraday cage. The charge and velocity can be calculated from the amplitude and width of the pulse. For this particular droplet the vertical voltage scale was —20 mv./cm. so the pulse amplitude was —56 mv. The magnitude of the charge on the droplet is given by $q = (C_{in})\ (V)/G$, where C_{in} is the total input capacitance to the grid of the cathode follower, V is the signal voltage measured on the oscilloscope, and G is the gain of the cathode follower. The input capacity was 4 $\mu\mu$f. and the gain of the cathode follower was 0.58; thus, the charge on the vertical droplet was -3.38×10^{-13} coulombs. The velocity of the droplet was the length of the Faraday cage, which was 1.08 cm., divided by the time the droplet spent in the cage. Since the horizontal time scale was 1 msec./cm., the time the droplet spent in the Faraday cage was approximately 3.3 msec. The velocity of the vertical droplet was thus calculated to be 328 cm./sec. In a similar manner the charge and velocity of the horizontal droplet were found to be 2.2×10^{-13} coulomb and 110 cm./sec. Figure 5 shows a sequence of photographs indicating the relative trajectory, collision, and coalescence of these two droplets. The larger droplet falling in the vertical direction was 96 μ in radius and the smaller droplet moving in the horizontal direction was 79 μ in radius. The time lapse between the first few photographs was determined from the calibrated delaying pulser and is indicated under the corresponding picture. The time calibration was not

[2] This assumes that the input resistance to the detector is high enough so that a significant amount of charge does not leak off the inner electrode while the droplet is passing through the electrode. In our case, the input resistance of the cathode follower was 10^{13} ohms.

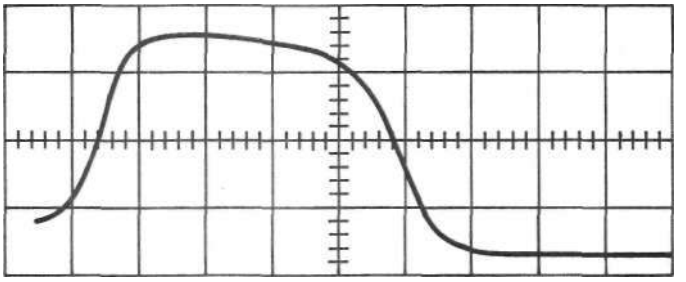

FIG. 4. Pulse from a charged droplet measured with the Faraday cage.

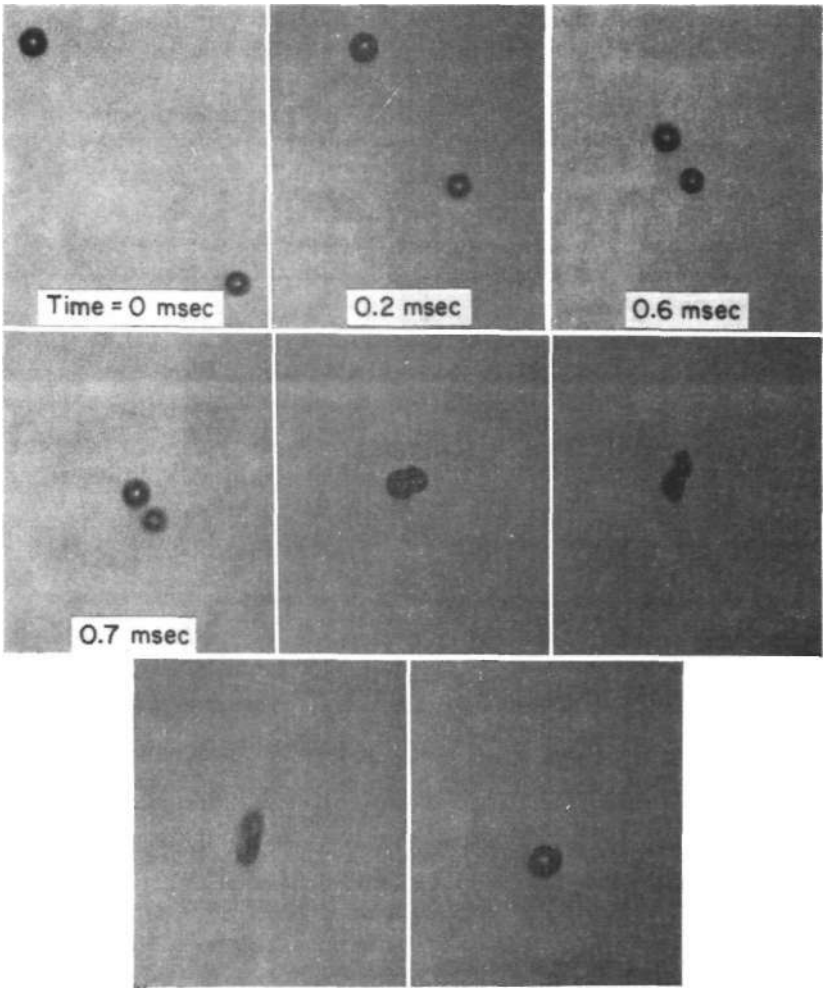

FIG. 5. The collision and coalescence of a 96 μ and a 79 μ droplet with opposite sign of charge.

accurate enough to yield a realistic determination of the time lapse between the other photographs.

A number of trajectories of highly charged droplets (10^{-13} coulomb) with opposite signs of charge were observed in the 4 X 5 camera under high magnification. The observations indicated that approximately 11 collisions were observed every 15 sec. or 110 collisions for 150 attempts. With this high a collision rate it was simple to photograph the collision and coalescence of two highly charged droplets with opposite signs of charge. Where the droplets were highly charged with the same sign of charge, approximately one collision was observed every 15 sec. or one collision for 150 attempts. One would expect a lower collision rate for these droplets because of the mutual electrostatic repulsion between them. However, at close distances an attraction force would exist if the droplets differed in size.

REFERENCES

1. BERG, T. G. O., FERNISH, G. C, AND GAULKER, T. A., *J. Atmos. Sci.* 20, 153 (1963).
2. PLUMLEE, H. R., Ph.D. dissertation, University of Illinois, 1964.
3. PROKHOROV, P. S., *Discussions Faraday Soc.* 18, 41 (1954).
4. LINDBLAD, N. It., *J. Colloid Sci.* 19, 729 (1964).
5. SCHNEIDER, J. M., AND HENDRICKS, C. D., *Rev. Sci. Inslr.* 35, 1349 (1904).
6. LINDBLAD, N. I!.., AND SCHNEIDER, J. M., Submitted for publication in the *J. Sci., Instr.* 1965.

DISCUSSION

WILLIAM H. FISCHER *(National Center for Atmospheric Research, Boulder, Colorado):* Are charge and mass conserved when drops ot like charge collide? If not, corona discharge may be occurring so that the incorrect relative drop charge is being plotted.

J. M. SCHNEIDER: Measurements are now underway which we hope will determine whether or not droplet charge is conserved in these collisions. However, we feel that the field surrounding the droplets we are presently using is insufficient to cause corona.

K. T. WHITBY *(University of Minnesota):* How was the water prepared for these experiments? In what kind of a container was the water stored?

J. M. SCHNEIDER: The water was double distilled and was stored in five gallon polyethylene bottles.

A. S. TEOT *(DOW Chemical Company, Midland, Michigan):* Do your delay times decrease when the charge difference on the two spheres is greater?

J. M. SCHNEIDER: For oppositely charged droplets there seems to be a linear relationship between the delay time and charge difference between the drops, the delay time decreasing with increasing charge difference. For droplets of like charge the curve seems rather strange and has as yet an unexplained dip in the delay time for slightly charged droplets.

T. GILLESPIE *(DOW Chemical Company, Midland, Michigan):* Was there a spread in the delay times?

J. M. SCHNEIDER: The spread was very small.

Reprinted from: Proc. of the Intern. Conf. on Cloud Physics,
Tokyo and Sapporo, Japan, May, 1965.

ON THE COALESCENCE AND COLLISION OF WATER DROPS[1]

Richard 0. Semonin and Hubert R. Plumlee
Illinois State Water Survey

1. INTRODUCTION

The study of the all-water process of precipitation formation has led to the concepts of coalescence, collision, and collection efficiencies between droplets of varying size. The collision efficiency is defined as the ratio of the area from which droplets will collide to the cross-section area of the target drop. The coalescence efficiency is the percentage of colliding droplets which merge to form a larger drop. The collection efficiency is the product of the collision and coalescence efficiencies.

One method of attempting to modify the droplet distribution within all-water clouds is to maximize these efficiencies. By the very definition of the coalescence efficiency, it can never exceed but may acquire any value less than or equal to unity. On the other hand, the collision efficiency theoretically is unlimited. The collision between a pair of droplets is determined by the trajectories of the droplets while subjected to gravitational and aerodynamical forces. If additional action-at-a-distance forces are present or introduced, a modification of the aerodynamic collision efficiency will result.

Thus, the problem lends itself to two essentially independent avenues of research. On the one hand, the forces necessary to alter the relative trajectory of a droplet pair must be investigated, and on the other hand the microphysics of the droplet surfaces must be studied to assure a maximum coalescence efficiency. The work reported here is an attempt to evaluate some of the possible forces and surface phenomena attendent to the maximization of the collection efficiency of water droplets.

2. THE COALESCENCE PROCESS

Through the use of light interference techniques, Derjaguin and Kussakov (1939) measured the distance between a flat plane and an approaching bubble and discovered that not only did the bubble flatten at a finite distance from the plane but that a dimple formed in the middle of the deformation. These findings supported a contemporary theory that the dynamics of the air film trapped between the surfaces determined the coalescence properties of the system. The thickness of the gap separating the colliding surfaces was again measured by the use of light interference patterns by Prokhorov (1954). He varied the humidity of the air around the liquid surfaces and found that for volatile liquids, if the humidity approached zero percent, the liquid surfaces would remain separated without coalescence for long periods of time. However, for 100 percent humidity, the surfaces would coalesce rapidly. Prokhorov concluded that the outflow of the vapor from the liquid surfaces created a hydrostatic pressure which prevented the surfaces from immediately merging together. He also verified that a dimple does form at the center of the deformed surfaces.

[1]The work reported herein was supported by the U. S. Army Electronic Research and Development Laboratory under grant AMC 63-G2 and National Science Foundation grant NSF GP-2528. The use of the IBM 7094 computer system was partially supported by National Science Foundation grant NSF GP-700.

Experiments described by Hendricks and Semonin (1962, 1963), similar to those of Prokhorov (1954), were carried out using distilled water with a conductivity of 10-6 mhos/cm. A pair of drops (hemispheres) were formed at the ends of two vertical brass tubes inside a hermetically sealed brass chamber. The separation between the tubes was adjusted so that as the drop3 were formed their surfaces would eventually come into contact. The rate of closure was governed by the rate of flow of water in the tubes. This was controlled by a constant speed motor which was set for two impact velocities of 76 μ/sec and 152 μ/sec.

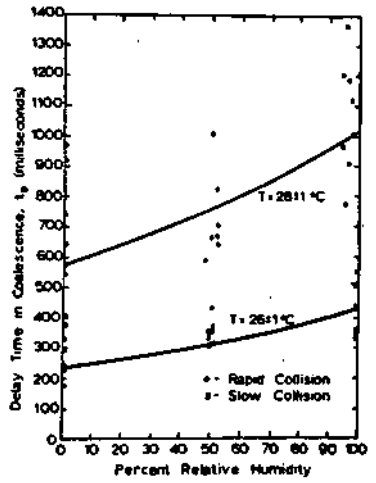

Fig. 1. Coalescence delay time as a function of relative humidity determined from Newton ring patterns.

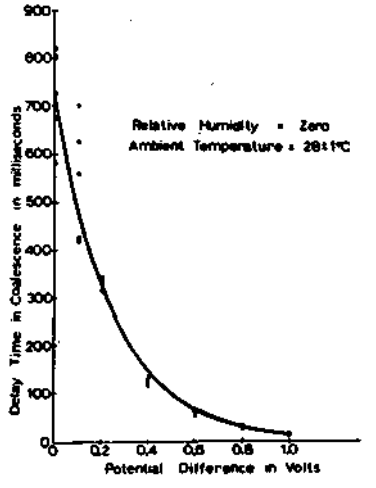

Fig. 2. Coalescence delay time as a function of voltage determined from Newton ring patterns.

The delay time before coalescence and the surface deformation of the two colliding drops were studied by photographing with a Fastax camera, at approximately 5000 frames per second, the changing interference patterns from a monochromatic light source reflected from the approaching surfaces. The effect of the environmental relative humidity on the delay time was determined at 0, 50 and 97 percent. The temperature during all experiments was at roan temperature. These results are shown in Figure 1.

The brass tubes containing the drops and the water sources were electrically isolated so that the effects of a potential difference between the surfaces could be investigated. A constant relative humidity of approximately zero percent was maintained in the drop chamber as the voltage between the drops was increased from 0 to 1 volt. The effect on the delay time of a voltage difference between the drops is shown in Figure 2.

A study of the profiles of colliding drop surfaces was undertaken to determine if the dimple reported by Prokhorov for various organic liquids could be detected for water. An example of the data is shown in Figure 3. The time zero for Figure 3a was determined as the time of the first flattening of the surfaces of the drops. The surface deformation at progressively later times is indicated in Figure 3b, c, d, and e. The final photograph, Figure 3f, which was the frame immediately following 3e, captured the coalescence process just prior to completion. The total delay time for this case was slightly greater than 624 milliseconds. These results were discussed in detail by Lindblad (1964). In every experiment, the dimple was noted, and in some instances when voltages were applied small protuberances were observed on the surfaces. The small protuberances may be due to the unstable growth of a random perturbation on the liquid surface as a result of the electric field between the drops.

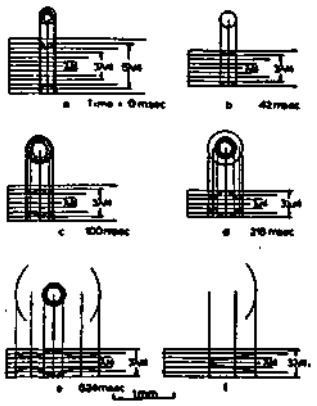

Fig. 3. Collision profiles deduced from Newton ring patterns.

A parallel experiment to obtain more estensive data on the delay time before coalescence, described by Plumlee (1964), was conducted by colliding a pair of drop3 suspended from hypodermic needles and photographing the profile of the collision with the high speed camera. A battery was connected so that a potential difference from 0 to 10 volts could be developed between the drops. A 10 ohm resistor was placed in series with the battery, and the voltage across the resistor was monitored with an oscilloscope. No voltage was observed, of course, until the two drop surfaces were in physical contact. When charge began to flow in the external circuit, a lamp was lighted and was photographed along the edge of the film. In this way the flow of charge was correlated with the visual coalescence. The results of these observations indicate that there is current between the drops prior to the visual coalescence. Since the voltage between the drops is inadequate to produce ionization of the air, it is hypothesized that the current is an indication of the initial transport of mass and is therefore the initiation of the coalescence process. These results are shown in Figure 4.

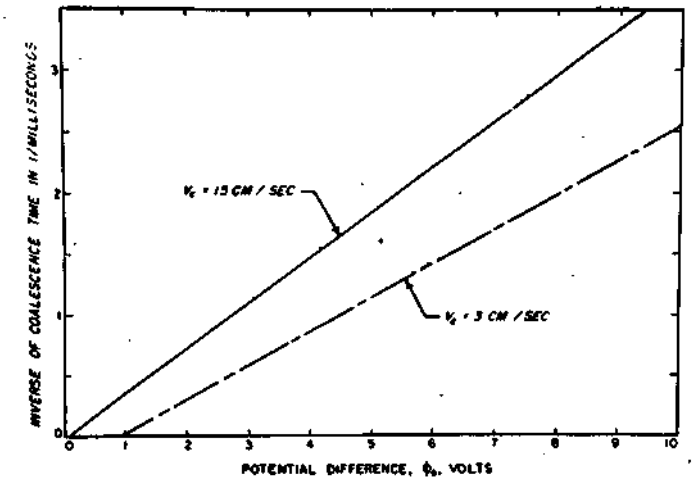

Fig. 4. Coalescence delay time as a function of voltage determined from collision profiles.

3. THE COLLISION PROCESS

In order that a pair of drops come into proximity for coalescence to take place a knowledge of the collision efficiency of various droplet pairs is necessary. Since the approach to the problem was primarily a theoretical one, it was possible to investigate sizes of droplets appropriate to many cumulus clouds. Studied were **the** effects of electric charge and fields on the collision

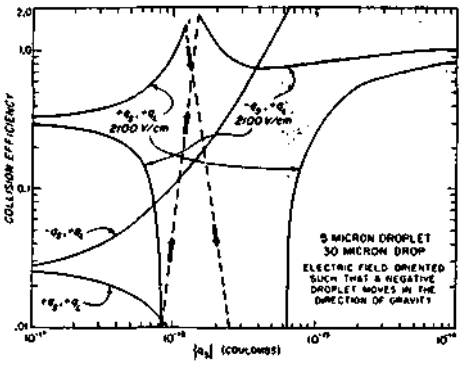

Fig. 5. Collision efficiencies for a 5 micron droplet with a 30 micron drop as a function of charge and electric field.

efficiencies of 5, 10, and 15 μ droplets paired in various combinations with drops of 30, 40, and 50 μ in radius. The results for a 5 and 30 μ drop pair are shown in Figure 5.

The effect of an electric field on the collision efficiency, not shown in Figure 5, always was such as to increase the value beyond that of the aerodynamical-gravitational efficiency. A thorough discussion of this effect was reported by Plumlee and Semonin (1965). This effect is suggested in Figure 5 by comparing the collision efficiencies for 5 μ droplets with charges, q_s, of 10^{-17} coulcmbs in the presence or absence of an electric field. The charge on the drop, q_L, was chosen as proportional to the ratio of the surface areas of the drop-droplet pair, and this charge was alvrays of positive sign. The efficiency was increased by a factor of 10 when an electric field of 2l00 volts/cm was applied.

Tn all of the cases, when charge of either sign was present on the drop-droplet pair, no noticeable effect on the collision efficiency was found until the charge on the droplet exceeded approximately 10^{-17} coulombs. As was expected, the collision efficiency increased rapidly with increasing charge when oppositely charged pairs were freely failing in the absence of an electric field. However, when the drop and droplet carried charges of the same sign, the efficiency decreased to zero with less than an order of magnitude increase in charge.

The effect of an electric field oriented such that positively charged droplets move in a direction opposite to the direction of gravity on charged pairs was quite opposed to intuition. For oppositely charged drop-droplet pairs in an applied field of 2100 volts/cm, the collision efficiency decreases to zero, which is similar tc the effect for a pair with the same sign of charge and no applied field. For a further increase of charge, however, the efficiency exceeds unity, then decreases, and finally increases to approximately unity. If the field is rotated 180° the collision efficiency does not tend to zero but continues to increase for charge magnitudes of up to 10^{-15} coulombs.

When the pairs were charged with the same sign of charge, the efficiency increased with increasing charge. For an additional increase in charge, the efficiency rose from zero and again appeared to approach unity. In both of these cases there was a region between 8.5 x 10~17 and 1.5 x 10-17 coulcmbs and between 1.2 x 10^{-16} and 2.0 x 10^{-16} coulombs for the oppositely charged and like charged pairs, respectively, which exceeded the capabilities of the digital computer program.

These results show that, when dealing with the growth of precipitation by a coalescence mechanism in clouds that are intensely electrified, the model must include the charge on the drop-drcplet pairs, the magnitude of the electric field, and the orientation of the electric field.

4. REFERENCES

Derjaguin, B., and M. Kussakov, 1939: Anomalous properties of thin polymolecular films, Acta Physicochlm, 10, 25-44

Hendricks, C. D., and R. G. Semonin, 1962: Investigation of Water droplet coalescence, Charged Particle Res. Lab. Report, Univ. of I11., Urbana, 29p.

Hendricks, C. D., and R. G. Semonin, 1963: Investigation of water droplet coalescence, Charged Particle P.es. Lab. Rep. No. CPRL-?-64, Univ. of I11., Urbana, 6lp.

Lindblad, N. R., 1964: Effects of relative humidity and electric charge on the coalescence of curved water surfaces, J. Colloid Sci., 19, 729-743.

Plrmlee, H. R., 1964: Effects of electrostatic forces on drop collision and coalescence in air, Charged Particle Res. Lab. Rep. No. CPRL-8-64, Univ. of I11., Urbana, lOlp.

Plumlee, H. R., and R. G. Semonin, 1965: Collision efficiency of charged cloud droplets in electric fields, accepted fcr publication in Tellus.

Prokhcrov, P. S., 1954: The effects of humidity deficit on coagulation processes and the coalescence of liquid drops, Discussions, Faraday Soc., 18. 41-51.

EFFECTS OF ELECTROSTATIC FORCES ON DROP COLLISION AND COALESCENCE IN AIR

BY
Hubert Russel Plumlee
25 September 1964

AMC-63-G2
NSF GP-2528

Supported by
ADVANCED RESEARCH PROJECTS AGENCY
and
NATIONAL SCIENCE FOUNDATION

Charged Particle Research Laboratory
Report No. CPRL-8-64
Department of Electrical Engineering
Engineering Experiment Station
University of Illinois
and
Illinois State Water Survey
Urbana, Illinois

ABSTRACT

The collision and coalescence of drops are studied with emphasis on the effects of electrostatic forces. A historical review is used to point out some of the earlier research in this field of study.

A mathematical model describing the effects of forces acting on two spherical drops immersed in a viscous medium is described. The model includes the interaction of the drops with an externally applied electric field and with any charge present. The collision efficiencies between pairs of drops ranging in size from 5 to 70 microns in radius are given as a result of computing the grazing trajectories of the smaller droplets relative to the larger drops. For a fixed droplet size, the collision efficiency is found to increase as the drop size is increased. However, applied electric fields produce increases in the collision efficiency for a given pair of drops. For example a horizontal electric field of 3600 volts per centimeter increases the collision efficiency of a 30 and 5 microns drop pair by a factor of 34.5. Also for a given pair of drops with charges of the same sign, the collision efficiency decreases to zero as the charges increase in a field-free region but increases in value when a vertically applied field is present. When the charges on a given drop pair are of opposite sign, the collision efficiency increases to values greater than unity as the charges are increased in a field-free region but may decrease in value when a vertically applied field is present.

The coalescence of a pair of drops 2 millimeters in radius immersed in air is investigated by first considering a mathematical model which includes the hydrodynamic flow of the air from between the two approaching surfaces, the effect of the flattening of the adjacent surfaces,and the effect of an

electric potential between the drops. With this model the time required for the surfaces to move a given distance is determined as a function of the viscosity of the air, and the potential difference. High speed photographs of the profile view of two colliding drops are used in support of this model. The time interval between the initial deformation of the approaching drops and their coalescence, the rate of growth of the flatten deformation of the adjacent surfaces, and the collision velocity of the drops are measured. It is found that the time for coalescence is independent of moderate charges in the air pressure, varies inversely with the potential difference, and decreases for an increase in the collision velocity. Also the time interval during which charge flows between the drops before they actually coalesce is investigated.

TABLE OF CONTENTS

LIST OF ILLUSTRATIONS vi

LIST OF SYMBOLS ix

CHAPTER I INTRODUCTION 1

CHAPTER II HISTORICAL REVIEW 4

2.1 Theoretical Aspects of Computing Collision Efficiencies . . . 4

2.1a Hydrodynamics 5
2.1b Electrostatics 7
2.1c Equations of Motion 8
2.1d Collision Efficiencies 9

2.2 Experimental Collision Efficiencies 11

2.2a Cloud Size Droplets 12
2.2b Scaled Model Droplets 14

2.3 Coalescence Experiments 15

CHAPTER III THEORETICAL MODEL FOR DETERMINING COLLISION EFFICIENCIES. . . . 20

3.1 Definition of Collision Efficiency 20
3.2 Hydrodynamics 22
3.3 Electrostatics 30
3.4 Equations of Motion 39

CHAPTER IV EFFECTS OF ELECTROSTATIC FORCES ON THE COLLISION EFFICIENCY OF A PAIR OF DROPS 43

4.1 Without Electrostatic Forces 43
4.2 With an Applied Electric Field 43
4.3 With a Net Electric Charge 52
4.4 With Both an Applied Electric Field and an Electric Charge. . . . 55

CHAPTER V THEORETICAL ASPECTS OF THE COALESCENCE PROCESS 63

5.1 The Coalescence Process 63
5.2 Trapped Gas Film Between the Colliding Surfaces 63
5.3 Effects of an Electric Potential Difference 68
5.4 Stability of the Liquid Surfaces 70

CHAPTER VI EXPERIMENTAL OBSERVATIONS OF THE COALESCENCE PROCESS 73

6.1 Experimental Technique 73
6.2 Effects of Electrostatic Forces on the Coalescence Process . . . 78

6.3 Effects of Pressure on the Coalescence Process 83
6.4 Charge Flow Before Coalescence 85
6.5 Rate of Growth of the Deformation 85

CHAPTER VII SUMMARY 90

7.1 Collision Efficiency of Drop Pairs 90
7.1a No Electrostatic Force 90
7.1b Electric Field Present. 90
7.1c Charged Drops 91
7.1d Charged Drops in an Electric Field 92

7.2 Coalescence of Drop Pairs 93
7.2a Effects of an Electric Potential Difference 93
7.2b Effects of Collision Velocity 93
7.2c Effects of Air Pressure 93
7.2d Charge Flow Before Coalescence 94
7.2e Rate of Growth of Deformation 94

7.3 Recommendations for Further Research 95

References 97

LIST OF ILLUSTRATIONS

Figure	Caption	Page
3-1	The grazing trajectories in the half-plane ($y > 0$ and $y < 0$) for a 30 micron drop and a 5 micron droplet in an electric field oriented at $\beta = 135°$.	21
3-2	Comparison of collision efficiency as calculated by various authors.	23
3-3	Illustration of the bispherical coordinate system.	33
3-4	Motion of a droplet in an electric field, E, relation to a fixed drop.	40
4-1	Collision efficiency curves when no electrostatic force is present.	44
4-2	Collision efficiency curves for a 30 micron drop with a 5, 10, and 12 micron droplet.	45
4-3	Collision efficiency curves for a 40 micron drop with a 5, 10, and 15 micron droplet.	46
4-4	Collision efficiency curves for a 50 micron drop with a 5, 10, and 15 micron droplet.	47
4-5	Trajectories for a 30 micron drop and a 5 micron droplet.	49
4-6	Change in collision efficiency of drop pairs for various orientations of electric field.	50
4-7	Change in collision efficiency of drop pairs for various orientations of electric fields at 3,000 volts per centimeter.	51
4-8	Collision efficiency curves for a 5 micron droplet with a 30, 40, and 50 micron drop.	53
4-9	Collision efficiency curves for a 10 micron droplet with a 30, 40, and 50 micron drop.	53
4-10	Collision efficiency curves for a 5 micron droplet with a 30, 40, and 50 micron drop.	54
4-11	Collision efficiency curves for a 10 micron droplet with a 30, 40, and 50 micron drop.	54

Figure	Caption	Page
4-12	Collision efficiency curves for a 30 micron and 5 micron drop pair with an electric field directed upward. $Q_\ell = 40 \lvert Q_s \rvert$	56
4-13	Collision efficiency curves for a 30 micron and 5 micron drop pair with an electric field directed downward. $Q_\ell = 40 \lvert Q_s \rvert$	56
4-14	Collision efficiency curves for a 30 micron and 5 micron drop pair with an electric field directed upward. $Q_\ell = 40 \lvert Q_s \rvert$	57
4-15	Collision efficiency curves for a 30 micron and 5 micron drop pair with an electric field directed upward. $Q_\ell = 40 \lvert Q_s \rvert$	57
4-16	Collision efficiency curves for a 40 micron and 5 micron drop pair with an electric field directed upward. $Q_\ell = 64 \lvert Q_s \rvert$	59
4-17	Collision efficiency curves for a 40 micron and 5 micron drop pair with an electric field directed downward. $Q_\ell = 64 \lvert Q_s \rvert$	59
4-18	Collision efficiency curves for a 40 micron and 5 micron drop pair with an electric field directed upward. $Q_\ell = 64 \lvert Q_s \rvert$	60
4-19	Collision efficiency curves for a 40 micron and 5 micron drop pair with an electric field directed downward. $Q_\ell = 64 \lvert Q_s \rvert$	60
4-20	Collision efficiency curves for a 50 and 5 micron drop pair with an electric field directed downward. $Q_\ell = 100 \lvert Q_s \rvert$	61
4-21	Collision efficiency curves for a 50 micron and 5 micron drop pair with an electric field directed downward. $Q_\ell = 100 \lvert Q_s \rvert$	61
4-22	Collision efficiency curves for a 50 micron and 5 micron drop pair with an electric field directed upward. $Q_\ell = 100 \lvert Q_s \rvert$	62
4-23	Collision efficiency curves for a 50 micron and 5 micron drop pair with an electric field directed downward. $Q_\ell = 100 \lvert Q_s \rvert$	62

Figure	Caption	Page
5-1	Illustration of the deformation of the adjacent surfaces of the colliding drops.	65
6-1	Block diagram of the experimental apparatus for measuring the current between colliding water drops.	75
6-2	Photographs showed the profile of two water drops before collision, after collision, and after coalescence.	77
6-3	A sequence of photographs taken at 14,000 frames per second of colliding and coalescing water drops at a potential difference of 1 volt.	79
6-4	A plot of the inverse of coalescence time as a function of the potential difference between drops.	80
6-5	A sequence of photographs taken at 14,000 frames per second of colliding and separating water drops with no potential difference.	81
6-6	A plot of the inverse of coalescence time as a function of the potential difference between drops for various air pressures, P.	84
6-7	A plot of the current time as a function of the potential difference between drops.	86
6-8	A plot of the height of the flattened surface of the collided drops as a function of time after contact.	87
6-9	A plot of the lense width as a function of time after coalescence.	89